On an extended clarifier-thickener model with singular source and sink terms

R. BÜRGER[1], A. GARCIA[1], K. H. KARLSEN[2] and J. D. TOWERS[3]

[1] *Departamento de Ingeniería Matemática, Facultad de Ciencias Físicas y Matemáticas,
Universidad de Concepción, Casilla 160-C, Concepción, Chile.*
email: `rburger@ing-mat.udec.cl`, `agarcia@ing-mat.udec.cl`
[2] *Centre of Mathematics for Applications (CMA), University of Oslo, P.O. Box 1053, Blindern,
N-0316 Oslo, Norway. email:* `kennethk@math.uio.no`
[3] *MiraCosta College, 3333 Manchester Avenue, Cardiff-by-the-Sea, CA 92007-1516, USA.*
email: `john.towers@cox.net`

A one-dimensional model of clarifier-thickener units in engineering applications can be expressed as a conservation law with a flux that is discontinuous with respect to the spatial variable. This model also includes a singular feed source. In this paper, the clarifier-thickener model studied in a previous paper (*Numer. Math.* **97** (2004) 25–65) is extended by a singular sink through which material is extracted from the unit. A difficulty is that in contrast to the singular source, the sink term cannot be incorporated into the flux function; rather, the sink is represented by a new non-conservative transport term. To focus on the new analytical difficulties arising due to this non-conservative term, a reduced problem is formulated, which contains the new sink term of the extended clarifier-thickener model, but not the source term and flux discontinuities. The paper is concerned with numerical methods for both models (extended and reduced) and with the well-posedness analysis for the reduced problem. For the reduced problem, a definition of entropy solutions, based on Kružkov-type entropy functions and fluxes, is provided. Jump conditions are derived and uniqueness of the entropy solution is shown. Existence of an entropy solution is shown by proving convergence of a monotone difference scheme. Two variants of the numerical scheme are introduced. Numerical examples illustrate that all three variants converge to the entropy solution, but introduce different amounts of numerical diffusion.

1 Introduction

1.1 Scope

In recent years there has been an increased interest in the analysis and numerics of conservation laws of the type $u_t + f(\gamma(x), u)_x = 0$, where $\gamma(x)$ is a vector of parameters that depend discontinuously on the spatial position x. This equation is the main ingredient of a clarifier-thickener model [9, 12, 14, 20], but also appears in other applications [8, 13, 17, 33, 42, 47, 49, 54]. We here study an extended clarifier-thickener model given by the equation

$$u_t + f(\gamma(x), u)_x = \gamma^3(x)u_x, \quad (x, t) \in \Pi_T := \mathbb{R} \times (0, T), \tag{1.1.1}$$

where $\gamma(x) = (\gamma^1(x), \gamma^2(x))$ is a vector of discontinuous parameters which correspond to singular feed sources and flux discontinuities. The discontinuous function $\gamma^3(x)$ is the transport coefficient of the non-conservative term $\gamma^3(x)u_x$, which represents a new singular sink that models the continuous extraction of material from the clarifier-thickener. The function γ^3 is a Heaviside-type function whose jump is located at the position of the sink. On the other hand, the functions γ^1 and γ^2 are continuous across the sink position. Since their discontinuities do not interfere with the sink, and we already know from [12] how to deal with them, we concentrate in this paper on an initial value problem for the reduced equation

$$u_t + \varphi(u)_x - \gamma(x)u_x = 0, \quad (x,t) \in \Pi_T. \tag{1.1.2}$$

Roughly speaking, the nonlinear function φ arises from evaluating $f(\gamma(x), u)$ at a fixed point of continuity of γ, and the remaining discontinuous coefficient γ represents γ^3 after the sink has been shifted to $x = 0$. We refer to (1.1.1) and (1.1.2) as the *full equation* and the *reduced equation*, respectively. Together with an initial condition and further assumptions on the nonlinearity of the flux and on the discontinuous coefficients, these equations form the *full extended clarifier-thickener model* (or, in short, *full model*) and the *reduced problem*, respectively.

In this paper, we introduce a definition of entropy solutions for the reduced problem, which consists of two separate Kružkov-type [39] integral inequalities for the two half-spaces on either side of $x = 0$. The solutions on both sides are coupled by a series of jump conditions. We then prove that these jump conditions ensure an L^1 stability property, which implies uniqueness of an entropy solution. We introduce an explicit finite difference scheme for the full model, which is the scheme analyzed in earlier work [12] extended by an upwind discretization of $\gamma^3(x)u_x$. We prove that the numerical solution remains in the interval $[0, 1]$, that the scheme is monotone, that it satisfies a time continuity property, and that, for the reduced problem, it converges to an entropy solution. Thus, the reduced problem is well posed. Numerical examples demonstrate that several variants of the scheme, which vary in their ease of implementation and level of non-diffusive resolution, converge to entropy solutions of both the reduced problem and the full model.

To put the treatment in the proper perspective, let us first recall some known results for the equation $u_t + f(\gamma(x), u)_x = 0$. The basic difficulty is that its well-posedness is not a straightforward limit case of the standard theory for conservation laws with a flux that depends smoothly on x. In fact, several extensions of the Kružkov entropy solution concept [39] to conservation laws with a discontinuous flux were proposed in recent years [1, 3, 4, 30, 31, 34, 36, 37, 38, 41, 50, 52, 53]. Each of these concepts is supported by a convergence analysis of a numerical scheme; the differences between them appear in the respective admissibility conditions for stationary jumps of the solution across the discontinuities of γ [10].

The choice of the entropy solution concept depends on the regularizing viscous physical model. For clarifier-thickener models, the appropriate concept emerges from the limit $\varepsilon \to 0$ of a viscous regularization εu_{xx} with a diffusion constant $\varepsilon > 0$ [14]. Thorough analyses and construction of exact entropy solutions for clarifier-thickener models were advanced by Diehl [19, 20, 21, 22, 23, 24]. On the other hand, the authors with collaborators

made a series of contributions [6, 9, 11, 12, 14, 15] to the well-posedness and numerical analysis for these models, whose basic non-standard ingredient is a singular feed source that produces diverging bulk flows, which causes the discontinuous x-dependence of the flux.

We may also write the reduced equation (1.1.2) as a non-strictly hyperbolic system

$$a_t = 0, \quad u_t + F(a, u)_x - G(a, u)a_x = 0, \quad x \in \mathbb{R}, \quad t \geqslant 0;$$
$$(a, u)(0, x) = \big(a_0(x), u_0(x)\big), \quad x \in \mathbb{R}, \tag{1.1.3}$$

where we define $a_0(x) := H(x)$, $G(a, u) := u$ and $F(a, u) := (q + a)u + b(u)$. In passing, we note that for $F(a, u) := f(a, u)$, $G \equiv 0$, and $a_0(x) := \gamma(x)$, (1.1.3) is equivalent to the Cauchy problem for $u_t + f(\gamma(x), u)_x = 0$ with a scalar discontinuous parameter $\gamma(x)$. The resulting triangular hyperbolic system has been the starting point of several analyses of this Cauchy problem [9, 21, 25, 30, 31, 37, 38].

Systems of the type (1.1.3) with $G \equiv 0$ were recently analyzed by Amadori et al. [2]. They solve the Riemann problem for (1.1.3), prove convergence of a Godunov scheme, and address uniqueness by a Kružkov-type technique. However, our reduced model is not a sub-case included in their analysis, since some of their structural assumptions are not satisfied in our case. For example, their requirement (P$_4$), stating that $F_a - G \neq 0$ for all (a, u) with $F_u(a, u) = 0$, is not satisfied, since $F_a - G \equiv 0$ in our case. We should point out that their uniqueness result does not hold for a discontinuous coefficient a, while our approach does include uniqueness.

1.2 Reduced problem and full model

The novel feature of our new extended clarifier-thickener model is a singular sink through which material may be extracted. The reduced problem emerges from the new model if the "unit" is assumed to have a sink only, but no sources, and is defined by the reduced equation (1.1.2) along with

$$u(x, 0) = u_0(x), \ x \in \mathbb{R}, \quad u_0 \in [0, u_{\max}], \ u_{\max} \in (0, 1], \tag{1.1.4}$$

$$\varphi(u) = qu + b(u), \quad \gamma(x) = \begin{cases} 0 & \text{for } x < 0, \\ \gamma_+ & \text{for } x > 0, \end{cases} \quad q \leqslant 0, \ \gamma_+ > 0. \tag{1.1.5}$$

Here, the function $b(u)$ is assumed to be Lipschitz continuous, positive for $u \in (0, 1)$, and to vanish for $u \notin (0, 1)$. We assume that $b(u)$ is twice differentiable in $(0, 1)$, that $b'(u) = 0$ at exactly one location $u = u_b^* \in (0, 1)$, where $b(u)$ has a maximum, and that $b''(u) = 0$ at no more than one inflection point $u_{\text{infl}} \in (0, 1)$; if such a point is present, we assume that $u_{\text{infl}} \in (u_b^*, 1)$. The restriction $q \leqslant 0$ is required in the stability and uniqueness analysis. See § 2 for a detailed derivation.

If we set $u_{\max} = 1$, then the assumptions on $b(u)$ are satisfied by the frequently used Richardson-Zaki [48] type function

$$b(u) = \begin{cases} v_\infty u(1 - u)^n & \text{for } u \in [0, u_{\max}], \\ 0 & \text{otherwise}, \end{cases} \quad n > 1, \quad v_\infty > 0, \tag{1.1.6}$$

where v_∞ is the settling velocity of a single particle in an unbounded medium. With the assumptions on $b(u)$ and the sign of q, the flux $\varphi(u)$ has a single maximum at $u^* \in [0, 1]$, and φ is non-decreasing on $[0, u^*]$ and non-increasing on $[u^*, 1]$.

The full model is defined by (1.1.1) along with the initial condition (1.1.4) and

$$f\big(\gamma(x), u\big) := \gamma^1(x) b(u) + \gamma^2(x)(u - u_F), \quad \gamma(x) := \big(\gamma^1(x), \gamma^2(x)\big), \tag{1.1.7}$$

$$\gamma^1(x) := \begin{cases} 0 & \text{for } x \notin [x_L, x_R], \\ 1 & \text{for } x \in [x_L, x_R], \end{cases} \quad \gamma^2(x) := \begin{cases} \tilde{q}_R - q_F & \text{for } x < 0, \\ \tilde{q}_R & \text{for } x > 0, \end{cases} \tag{1.1.8}$$

where u_F denotes the feed concentration, $x_L < x_D < 0 < x_R$ are the overflow, sink, and discharge levels, respectively, reflecting the design of the unit, and $\tilde{q}_R < 0$ and $q_F > 0$ are given bulk flow velocities describing operating conditions. Thus, $f(\gamma(x), u)$ incorporates the batch flux, the source term, and the discontinuities at the discharge and overflow levels. (The precise meaning of all variables is given in § 2.) Finally, the discontinuous transport coefficient $\gamma^3(x)$ is given by

$$\gamma^3(x) := \begin{cases} 0 & \text{for } x < x_D, \\ -q_D > 0 & \text{for } x > x_D, \end{cases} \tag{1.1.9}$$

where $q_D < 0$ is another velocity related to sink control (see Section 2). Observe that the full model is defined by a conservation law with a flux that is discontinuous at the source and transition points, but *not* at the location of the singular sink.

1.3 Outline of the paper

The remainder of this paper is organized as follows. The full extended clarifier-thickener model and the reduced problem are derived in § 2. For the reduced problem, we present in § 3 the definition of entropy solutions and, using the jump conditions, establish an L^1 stability property, which implies uniqueness of an entropy solution.

In § 4, we introduce an explicit finite difference scheme for the full model, and prove that the numerical solution remains in the interval $[0, 1]$, that the scheme is monotone, and that it satisfies a time continuity property. In § 5 we focus on the reduced problem and prove that the scheme satisfies a spatial variation bound. Starting from a discrete entropy inequality, using the monotonicity and proceeding as in the proof of the Lax-Wendroff theorem, we then show that the scheme converges to an entropy solution of the reduced problem. The analysis is summarized in Theorem 5.1 stating the well-posedness of the reduced problem.

Several suitable schemes for the reduced or full equation can be formulated by combining upwind discretizations for the linear terms with an Engquist-Osher type numerical flux for the remaining nonlinear portion. Based on this observation, we introduce in § 6 two different variants of our scheme, which are referred to as "Scheme 1" and "Scheme 3", respectively, while the scheme analyzed so far is called "Scheme 2". (This nomenclature anticipates the observed ranking in performance.) The analysis of Scheme 2 in § 4 and § 5 also fully holds for Scheme 1. The convergence result also applies to Scheme 3, while

the entropy analysis may require different arguments. Numerical examples for the three schemes are presented in §7 for both the reduced problem and the complete model.

§8 collects some conclusions that can be drawn from our well-posedness and numerical analysis. Moreover, we comment on the numerical results of §7. It turns out that although all three schemes converge to the entropy solution, they significantly differ in the degree of numerical diffusion introduced. Scheme 1 is very easy to implement, but turns out to be very diffusive, especially for steady-state, while Scheme 3 produces sharp resolution.

2 The extended clarifier-thickener model

2.1 Clarifier-thickener models, singular sources, and singular sinks

Clarifier-thickener units are widely used in chemical engineering, wastewater treatment, mineral processing and other applications to separate a suspension of finely divided solid particles dispersed in a viscous fluid into its solid and liquid components. The basic clarifier-thickener model can be derived from the scalar conservation law

$$u_t + b(u)_x = 0, \quad x \in [0, L], \quad t > 0; \quad u(x, 0) = u_0(x), \quad x \in [0, L] \qquad (2.2.1)$$

of the kinematic sedimentation model [16, 40], which describes the settling of a suspension of initial concentration $u_0(x)$ in a settling vessel of height L. Here, u is the sought concentration as a function of depth x and time t, and $b(u)$ is the hindered settling function or batch flux density function, which is a material-dependent function. A typical example is the function (1.1.6).

We emphasize that all manipulations performed herein to derive the final form of the governing equation are made under the assumption that the solution u is smooth. Of course, solutions to nonlinear conservation laws like (2.2.1) and all partial differential equations that follow within this section are discontinuous in general. However, we provide an appropiate concept of discontinuous solutions, including an entropy concept to ensure uniqueness, for the final model only (see Definition 3.1 in §3).

Suppose now that we pump the suspension into a vertical tube that is filled with water at a feed level $x = 0$, and that part of the mixture flows upwards at velocity $q_L < 0$, while the remainder flows downwards at velocity $q_R > 0$, as in the left diagram of Figure 1. Consequently, if $\mathscr{S}$ is the cross-sectional area of the tube, then $Q_F = (q_R - q_L)\mathscr{S}$. Assuming for a moment that we inject only clear water at $x = 0$, we obtain the conservation law with discontinuous flux

$$u_t + \big(q(x)u + b(u)\big)_x = 0, \quad q(x) := \begin{cases} q_L < 0 & \text{for } x < 0, \\ q_R > 0 & \text{for } x > 0. \end{cases} \qquad (2.2.2)$$

Now let us inject feed suspension of a given concentration u_F at a volume rate Q_F. Since the feed source is concentrated at $x = 0$, we need to add the singular source term $\delta(x)(q_R - q_L)u_F$ to the right-hand side of the equation in (2.2.2), obtaining

$$u_t + \big(q(x)u + b(u)\big)_x = \delta(x)(q_R - q_L)u_F. \qquad (2.2.3)$$
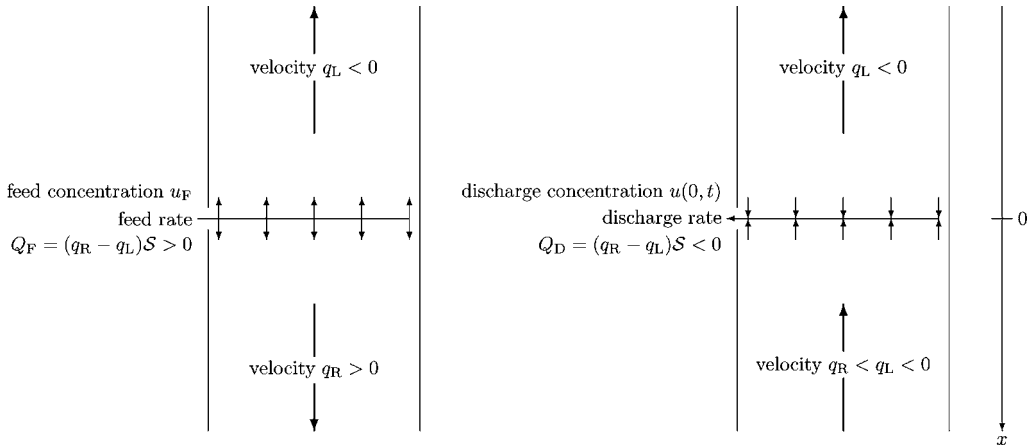
FIGURE 1. Basic flow variables for a singular source term (left) and a singular sink term (right).

However, using the Heaviside function $H(x)$, we may formally write

$$\delta(x)(q_R - q_L)u_F = \big(H(x)(q_R - q_L)u_F\big)_x.$$

Then (2.2.3) assumes the form

$$u_t + \Big(q(x)u + b(u) - \big(H(x)(q_R - q_L)u_F\big)\Big)_x = 0, \tag{2.2.4}$$

so that the singular source is expressed as a discontinuity of the flux function. This is possible since u_F is a *given* constant (or possibly a given (control) function of t). Thus, the governing conservation law can be written as

$$u_t + g(u, x)_x = 0, \quad g(u, x) := \begin{cases} q_L(u - u_F) + b(u) & \text{for } x < 0, \\ q_R(u - u_F) + b(u) & \text{for } x \geqslant 0. \end{cases} \tag{2.2.5}$$

Note that the *injection* of material of given concentration and at given rate leads to a homogeneous conservation law with discontinuous flux. This property has made the clarifier-thickener model tractable.

In the present work, we extend the clarifier-thickener model to the case that we also extract material at a fixed location. To elucidate the problem, consider a column with an upwards directed bulk flow of $Q_R < 0$. At depth $x = 0$, we divide the flow into a discharge flow $Q_D < 0$ and the remaining upwards directed bulk flow Q_L with $Q_R < Q_L < 0$, see the right diagram of Figure 1. Considering that the concentration $u(0, t)$ of the suspension extracted is unknown beforehand and defining $q_R := Q_R/\mathscr{S}$ and $q_L := Q_L/\mathscr{S}$, we obtain instead of (2.2.5) the equation

$$u_t + h(u, x)_x = \delta(x)(q_R - q_L)u(x, t), \quad h(u, x) = \begin{cases} q_L u + b(u) & \text{for } x < 0, \\ q_R u + b(u) & \text{for } x > 0. \end{cases} \tag{2.2.6}$$

Note that we cannot use the Heaviside function in the same way as in (2.2.4), since now the solution value $u(x,t)$ replaces the constant u_F in the singular term. This difference justifies studying the sink term problem in its own right, rather than claiming that it is just analogous to the source term problem. This view is further supported by the observation that the so-called crossing condition [35], which ensures uniqueness of an entropy solution of the initial value problem, is satisfied for (2.2.5) but may be violated for (2.2.6), so uniqueness is not obvious here.

Note that the right-hand side of (2.2.6) includes a δ function multiplying the function $u(x,t)$, which will be discontinuous in general. In other words, we have a non-conservative product in (2.2.6), which is potentially ill-defined for the discontinuous solutions we are ultimately interested in. However, since we are still in the stage of model development, we will not deal with this problem here. In fact, the "$\delta(x) \cdot u(x,t)$"-type non-conservative product will be manipulated further on in §2.3 by a "differentiation by parts", for which a detailed justification is provided; finally, our solution concept stated in Section 3 incorporates this non-conservative product in a precisely defined way.

Finally, let us mention that several researchers in chemical engineering and mineral processing have reported experiments with separation devices that can be modelled by the extended clarifier-thickener concept by possibly considering several discharge sink terms located at different depths. (It is clear that if we know how to properly handle one sink term, then we can also deal with any array of them.) References to experimental information include [27, 28, 29, 43, 44, 45, 46, 51].

2.2 Bulk flow variables

Consider the extended clarifier-thickener drawn in Figure 2, which is supposed to have a constant cross-sectional area $\mathscr{S}$. This setup is similar to that considered earlier [9, 11, 12], but is equipped with an additional sink located at depth x_D. This (of course, idealized) unit is operated as follows.

At $x = 0$, suspension is fed into the unit at a volume rate $Q_F(t) \geqslant 0$. The feed suspension is loaded with solids of the volume fraction $u_F(t) \in [0, u_{max}]$, where u_{max} is a maximum solids concentration. At $x = 0$, the feed flow divides into an upwards-directed and a downwards-directed bulk flow. We also prescribe the underflow volume rate $Q_R(t) \geqslant 0$ with $Q_R(t) \leqslant Q_F(t)$. Thus, the signed volume rate of the upwards-directed bulk flow immediately above the feed source is

$$Q_M(t) = Q_R(t) - Q_F(t) \leqslant 0. \tag{2.2.7}$$

At depth $x = x_D$, $x_L < x_D < 0$, a discharge sink is located. Suspension is extracted from the column at a signed volume rate $Q_D(t) \leqslant 0$, where we assume $Q_D(t) \geqslant Q_M(t)$. Above the discharge sink, for $x_L \leqslant x \leqslant x_D$, there is an upwards directed bulk flow with the volume rate

$$Q_L(t) = Q_M(t) - Q_D(t) = Q_R(t) - Q_F(t) - Q_D(t) \leqslant 0. \tag{2.2.8}$$

Summarizing, we prescribe the volume rates $Q_F(t)$, $Q_R(t)$ and $Q_D(t)$ and the feed
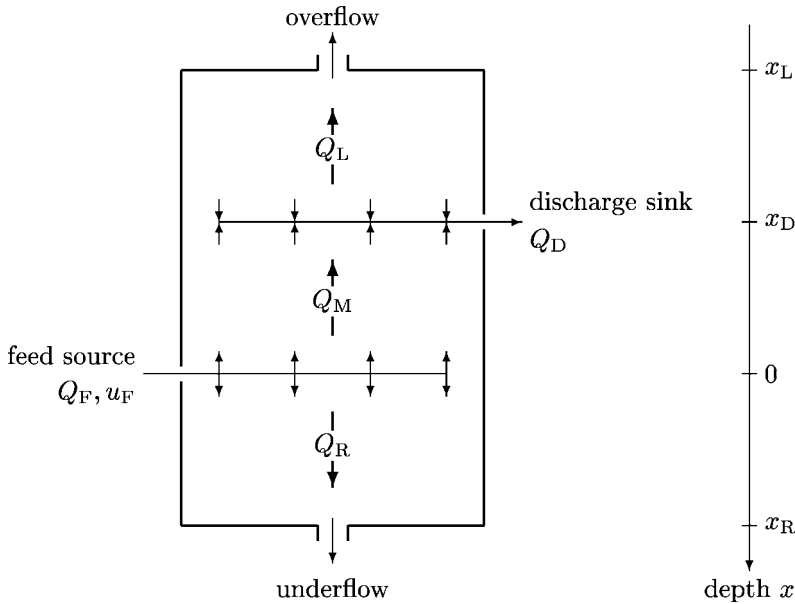
FIGURE 2. The extended clarifier-thickener setup showing the known bulk flows and control variables.

concentration $u_F(t)$ as independent control variables. From these we calculate the dependent control variables $Q_M(t)$ and $Q_L(t)$ by (2.2.7) and (2.2.8), respectively.

For the remainder of the paper, we assume that all control variables are constant, and introduce the velocities $q_c := Q_c/\mathscr{S}$, $c \in \{D, F, L, M, R\}$. Disregarding for a moment the solids sources and sinks but taking into account the bulk flows and utilizing independent control variables only, we can write the flux function as

$$\tilde{g}(u,x) = \begin{cases} (q_R - q_F - q_D)u & \text{for } x \leqslant x_L, \\ (q_R - q_F - q_D)u + b(u) & \text{for } x_L < x \leqslant x_D, \\ (q_R - q_F)u + b(u) & \text{for } x_D < x \leqslant 0, \\ q_R u + b(u) & \text{for } 0 < x \leqslant x_R, \\ q_R u & \text{for } x > x_R. \end{cases} \quad (2.2.9)$$

2.3 Solids feed and sink terms

Including now the solids feed and sink mechanisms, we obtain the conservation law with source terms

$$\begin{aligned} u_t + \tilde{g}(u,x)_x &= q_F u_F \delta(x) + q_D u(x,t)\delta(x - x_D) \\ &= q_F u_F H'(x) + q_D\big(H(x - x_D)u(x,t)\big)_x - q_D H(x - x_D)u_x(x,t), \end{aligned} \quad (2.2.10)$$

where $\delta(\cdot)$ denotes the Dirac delta mass. Observe that the differentiation by parts used here,

$$u(x,t)\delta(x - x_D) = \big(H(x - x_D)u(x,t)\big)_x - H(x - x_D)u_x(x,t),$$

is not defined in the sense of distributions. However, we continue to use the second equality in (2.2.10) as the defining equation of the extended clarifier-thickener model. This is supported by the integral version of the balance law, and the desired effect of the singular sink. Namely, if we fix $a \in (x_L, x_D)$ and $b \in (x_D, 0)$, so that $x_D \in [a,b]$ and define the total amount of solids

$$U_{[a,b]}(t) := \int_a^b u(x,t)\,dx,$$

then the rate of change of $U_{[a,b]}(t)$ should be given by the solids flux through $x = a$ minus the flux through $x = b$ minus the rate at which solids are extracted through $x = x_D$. However, integrating the second equality in (2.2.10) over $[a,b]$, taking into account the definition of $g(x,u)$ and assuming that the solution is smooth, we obtain

$$\begin{aligned}
U'_{[a,b]}(t) &= -\big(\tilde{g}(u(b,t),b) - \tilde{g}(u(a,t),a)\big)\\
&\quad + q_D H(b - x_D)u(b,t) - q_D H(a - x_D)u(a,t)\\
&\quad - q_D \int_a^b H(x - x_D)u_x(x,t)\,dx\\
&= -\big(\tilde{g}(u(b,t),b) - \tilde{g}(u(a,t),a)\big) + q_D u(b,t)\\
&\quad - q_D \int_{x_D}^b u_x(x,t)\,dx\\
&= \tilde{g}(u(a,t),a) - \tilde{g}(u(b,t),b) + q_D u(x_D,t),
\end{aligned}$$

which ensures equivalence at least at the level of smooth solutions between the first equation of (2.2.10) and the full extended clarifier-thickener model (1.1.1).

Note that even for smooth solutions, it is not possible to fully include the term $q_D u(x,t)\delta(x - x_D)$, or its equivalent obtained after differentiation by parts, into the flux term (which is differentiated with respect to x) on the left-hand side of (2.2.10). Thus, the problem cannot be written in standard conservation form.

Next, absorbing the term $q_F u_F H'(x) + q_D(H(x - x_D)u(x,t))_x$ into the convective flux yields the equation

$$u_t + g(u,x)_x = -q_D H(x - x_D)u_x(x,t), \tag{2.2.11}$$

where, after defining $\tilde{q}_R := q_R - q_D$ and adding $-q_L u_F$, we obtain the flux function

$$g(u,x) = \begin{cases}
(\tilde{q}_R - q_F)(u - u_F) & \text{for } x \leqslant x_L,\\
(\tilde{q}_R - q_F)(u - u_F) + b(u) & \text{for } x_L < x \leqslant 0,\\
\tilde{q}_R(u - u_F) + b(u) & \text{for } 0 < x \leqslant x_R,\\
\tilde{q}_R(u - u_F) & \text{for } x > x_R,
\end{cases} \tag{2.2.12}$$

which is continuous across $x = x_D$. Defining the discontinuous parameters $\gamma^1(x)$, $\gamma^2(x)$ and $\gamma^3(x)$ via (1.1.8) and (1.1.9) yields $g(u, x) = f(\gamma(x), u)$, where $f(\gamma(x), u)$ is defined by (1.1.7), so that the governing balance law (2.2.11) takes the final form (1.1.1).

2.4 Reduced problem

The analysis in this paper is focused on the reduced problem (1.1.2), (1.1.4), (1.1.5), which emerges from the model derived above if we consider only the vicinity of the sink term and assume that the velocities have been normalized such that q_D (in the original problem description) equals $-\gamma_+$, and that $q \leqslant 0$. Recall that we refer to (1.1.2), (1.1.4), (1.1.5) as *reduced problem*, while (1.1.1), (1.1.4), and (1.1.7)–(1.1.9) form the *full extended clarifier-thickener model* (in short, *full model*).

3 Entropy solution and uniqueness analysis of the reduced problem

Before stating the definition of entropy solution, we recall the notation $a \vee b := \max\{a, b\}$, $a \wedge b := \min\{a, b\}$. Also, we use the notation $\mathscr{D}(\Pi_T)$ to denote the set of test functions; $\mathscr{D}(\Pi_T) = C_c^\infty(\Pi_T)$.

Definition 3.1 (Entropy solution) *A function* $u : \Pi_T \mapsto \mathbb{R}$ *is an entropy solution of the initial value problem* (1.1.2), (1.1.4), (1.1.5) *if it satisfies the following conditions:*

(D.1) $u \in L^1(\Pi_T) \cap BV(\Pi_T)$ *and* $u(x, t) \in [0, 1]$ *for a.e.* $(x, t) \in \Pi_T$.

(D.2) *If* $0 \leqslant \psi \in \mathscr{D}(\Pi_T)$ *vanishes for* $x > 0$, *then*

$$\iint_{\Pi_T} \left(|u - c| \psi_t + \operatorname{sgn}(u - c)(\varphi(u) - \varphi(c))\psi_x \right) dt\, dx \geqslant 0 \quad \forall c \in \mathbb{R}, \tag{3.3.1}$$

and if $0 \leqslant \psi \in \mathscr{D}(\Pi_T)$ *vanishes for* $x < 0$, *then*

$$\iint_{\Pi_T} \left(|u - c| \psi_t + \operatorname{sgn}(u - c)(\varphi(u) - \varphi(c) - \gamma_+(u - c))\psi_x \right) dt\, dx \geqslant 0 \quad \forall c \in \mathbb{R}. \tag{3.3.2}$$

(D.3) *With the abbreviation* $u_\pm = u(0\pm, t)$, *the following jump conditions hold at* $x = 0$ *for a.e.* $t \in (0, T)$: *if* $u_- \leqslant c \leqslant u_+$, *then*

$$\varphi(u_+) - \varphi(c) \leqslant \gamma_+(u_+ - c), \tag{3.3.3}$$

$$\varphi(u_-) - \varphi(c) \leqslant 0, \tag{3.3.4}$$

and if $u_- \geqslant c \geqslant u_+$, *then*

$$\varphi(u_+) - \varphi(c) \geqslant \gamma_+(u_+ - c), \tag{3.3.5}$$

$$\varphi(u_-) - \varphi(c) \geqslant 0. \tag{3.3.6}$$

(D.4) *The initial condition is satisfied in the following strong* L^1 *sense:*

$$\operatorname*{ess\,lim}_{t \downarrow 0} \int_{\mathbb{R}} |u(x, t) - u_0(x)|\, dx = 0. \tag{3.3.7}$$

Remark 3.1 For the full extended clarifier-thickener model captured by equation (1.1.1), we would have to replace the condition $u \in BV(\Pi_T)$ by the weaker condition $u \in BV_t(\Pi_T)$. Here $BV_t(\Pi_T)$ is the class of functions $W(x, t)$ with $\partial_t W$ being a finite measure. The presence of the discontinuities in the parameter vector γ makes it difficult (in the case of the extended model (1.1.1)) to get global control of the spatial variation of the solution u.

Remark 3.2 It is clear from (3.3.1), (3.3.2) that if u is an entropy solution in the sense of Definition 3.1, then for $x < 0$, u is an entropy solution in the usual Kružkov sense of the conservation law $u_t + \varphi(u)_x = 0$, while for $x > 0$, u is an entropy solution (in the usual Kružkov sense) of the conservation law $u_t + (\varphi(u) - \gamma_+ u)_x = 0$.

Remark 3.3 The reduced equation (1.1.2) has a so-called non-conservative product. More specifically, we have what amounts to a δ function, u_x, multiplied by a discontinuous function $\gamma(x)$. We expect a jump condition of the form

$$\varphi(u_+) - \varphi(u_-) = \bar{\gamma}(u_+ - u_-), \tag{3.3.8}$$

where $\bar{\gamma}$ is some intermediate value of γ, i.e. $0 = \gamma_- \leqslant \bar{\gamma} \leqslant \gamma_+$. In fact, when $u_- \leqslant u_+$, we can take $c = u_-$ in (3.3.3) and then $c = u_+$ in (3.3.4) to get

$$0 \leqslant \varphi(u_+) - \varphi(u_-) \leqslant \gamma_+(u_+ - u_-),$$

which implies (3.3.8). Similarly, when $u_- \geqslant u_+$, we can take $c = u_-$ in (3.3.5) and then $c = u_+$ in (3.3.6) to get

$$\gamma_+(u_+ - u_-) \leqslant \varphi(u_+) - \varphi(u_-) \leqslant 0,$$

which again implies (3.3.8).

From the jump conditions in Definition 3.1 we derive the following additional jump conditions.

Lemma 3.1 *Let u be an entropy solution of the reduced problem in the sense of Definition 3.1. The following jump conditions hold at $x = 0$ for a.e. $t \in (0, T)$ for which $u_-(t) \neq u_+(t)$:*

$$0 \leqslant \frac{\varphi(u_+) - \varphi(u_-)}{u_+ - u_-} \leqslant \gamma_+, \tag{3.3.9}$$

$$u_+ < u_- \Rightarrow u_+ < u_- \leqslant u^*, \tag{3.3.10}$$

where u^* is the single maximum of $\varphi(u)$ (see §1.2).

Proof To prove (3.3.9), first take the case where $u_- < u_+$. Letting $c = u_-$ in (3.3.3), and then $c = u_+$ in (3.3.4), yields the inequalities

$$\varphi(u_+) - \varphi(u_-) \leqslant \gamma_+(u_+ - u_-), \quad \varphi(u_+) - \varphi(u_-) \geqslant 0,$$

which imply inequality (3.3.9). If $u_+ < u_-$, we arrive at (3.3.9) by a similar calculation, this time taking $c = u_-$ in (3.3.5), and then $c = u_+$ in (3.3.6).

To prove (3.3.10), it suffices to show that neither of the orderings $u_+ \leqslant u^* < u_-$, $u^* < u_+ < u_-$ is possible. If $u_+ \leqslant u^* < u_-$, letting $c = u^*$ in (3.3.6) results in $\varphi(u^*) - \varphi(u_-) \leqslant 0$, which contradicts our assumptions about the shape of the graph of $u \mapsto \varphi(u)$. If $u^* < u_+ < u_-$, letting $c = u^+$ in (3.3.6) yields $\varphi(u_+) - \varphi(u_-) \leqslant 0$. Since φ is strictly decreasing on $[u^*, 1]$, this is a contradiction.   □

Remark 3.4 In the absence of the sink term ($\gamma_+ = 0$), the jump condition (3.3.9) becomes

$$\frac{\varphi(u_+) - \varphi(u_-)}{u_+ - u_-} = 0,$$

which is the usual Rankine-Hugoniot condition satisfied by a zero-speed discontinuity for the conservation law $u_t + \varphi(u)_x = 0$. Based on this observation, it seems that (3.3.9) is playing the role of a Rankine-Hugoniot condition for a steady jump located at $x = 0$ where the delta-function due to the sink term is concentrated. Maintaining for the moment our focus on the situation where $\gamma_+ = 0$, the shape of the flux function $u \mapsto \varphi(u)$, along with the Rankine-Hugoniot condition, $\varphi(u_+) = \varphi(u_-)$, requires that u^* lies between u_- and u_+. It follows from (3.3.10) that in this situation $u_- < u^* < u_+$ if $u_- \neq u_+$. Thus when $\gamma_+ = 0$, the local entropy condition implied by the jump conditions (**D**.3) is the classical Lax condition for a steady shock.

Remark 3.5 If we set $\varphi \equiv 0$, the partial differential equation (1.1.2) reduces to

$$u_t - \gamma(x)u_x = 0, \tag{3.3.11}$$

a simple transport equation. Note that due to the form of the coefficient $\gamma(x)$, the interface values $u(0_-, t)$ and $u(0_+, t)$ are determined by the initial data alone, i.e., no interface conditions are required. Indeed, in the limiting case where φ vanishes, our jump conditions at $x = 0$ are satisfied trivially, i.e., they impose no restrictions on u_- and u_+. Using (3.3.1), (3.3.2) and (3.3.7), we find that the solution to (3.3.11) that is dictated by our definition of entropy solution is

$$u(x,t) = \begin{cases} u_0(x) & \text{for } x < 0, \\ u_0(x + \gamma_+ t) & \text{for } x > 0, \end{cases} \tag{3.3.12}$$

as expected from the form of (3.3.11) and the definition of γ. We refer the reader to the work of Bouchut & James [7] for a detailed study of linear transport equations with discontinuous coefficients such as (3.3.11). Note that (3.3.11) can be written in the form of [7, Eq. (1.1)], $u_t + a(x)u_x = 0$, if we define $a(x) = -\gamma(x)$. In view of our definition of $\gamma(x)$, (1.1.5), the function $a(x)$ is then piecewise constant with one decreasing jump. Thus, the one-sided Lipschitz condition [7, (1.8)] is trivially satisfied, and our solution (3.3.12) of (3.3.11) is also a solution in the sense of Bouchut & James [7].

We are now ready to prove that entropy solutions are L^1 stable and hence unique.

Theorem 3.1 (L^1 stability and uniqueness) *Let u and v be two entropy solutions in the sense of Definition 3.1 of the initial value problem* (1.1.2), (1.1.4), (1.1.5) *with initial data u_0 and v_0, respectively. Then, for a.e. $t \in (0, T)$,*

$$\int_{\mathbb{R}} |u(x, t) - v(x, t)| \, dx \leqslant \int_{\mathbb{R}} |u_0(x) - v_0(x)| \, dx.$$

In particular, there exists at most one entropy solution of the reduced model (1.1.2), (1.1.4), (1.1.5).

Proof Using standard methods and in particular the doubling of variables technique [39], one can derive from (3.3.1) and (3.3.2) the following pair of integral inequalities for u and v:

$$\forall \psi^1 \in \mathscr{D}(\Pi_T), \quad \psi^1(x, t) = 0 \text{ for } x > 0:$$
$$\iint_{\Pi_T} \left(|u - v| \psi_t^1 + \mathrm{sgn}(u - v) (\varphi(u) - \varphi(v)) \psi_x^1 \right) dt \, dx \geqslant 0, \tag{3.3.13}$$

$$\forall \psi^2 \in \mathscr{D}(\Pi_T), \quad \psi^2(x, t) = 0 \text{ for } x < 0:$$
$$\iint_{\Pi_T} \left(|u - v| \psi_t^2 + \mathrm{sgn}(u - v) (\varphi(u) - \varphi(v) - \gamma_+(u - v)) \psi_x^2 \right) dt \, dx \geqslant 0. \tag{3.3.14}$$

An approximation argument reveals that we may choose $\psi^1(x, t) = \Phi(t) v_h(x)$ and $\psi^2(x, t) = \Phi(t) \mu_h(x)$, where $\Phi \in C_0^2(0, T)$, $\Phi(\cdot) \geqslant 0$, and $\{\mu_h\}_{h>0}$ and $\{v_h\}_{h>0}$ are standard boundary layer sequences that are assumed to satisfy $\mu_h \in C^1(\mathbb{R})$, $\mu_h(x) = 0$ for $x \leqslant 0$, $0 \leqslant \mu_h(\cdot) \leqslant 1$, $\mu_h(x) = 1$ for $x > h$, $|\mu_h'(\cdot)| \leqslant C/h$, where C is a constant independent of h, and $v_h(x) := 1 - \mu_h(x + h)$. Since the solutions u and v possess traces with respect to $x \to 0$, we obtain by inserting ψ^1 and ψ^2 in (3.3.13) and (3.3.14), letting $h \to 0$, and using that for all h, ψ^1 vanishes for $x \geqslant 0$, while ψ^2 vanishes for $x \leqslant 0$, the inequalities

$$\int_{-\infty}^0 \int_0^T |u - v| \Phi'(t) \, dt \, dx$$
$$\geqslant \int_0^T \mathrm{sgn}(v_- - u_-) (\varphi(v_-) - \varphi(u_-)) \Phi(t) \, dt, \tag{3.3.15}$$

$$\int_0^\infty \int_0^T |u - v| \Phi'(t) \, dt \, dx$$
$$\geqslant -\int_0^T \mathrm{sgn}(v_+ - u_+) (\varphi(v_+) - \varphi(u_+) - \gamma_+(v_+ - u_+)) \Phi(t) \, dt. \tag{3.3.16}$$

In a standard fashion, let now ω_h be a non-negative C^∞ mollifier with support on $(-h, h)$ and $\|\omega_h\|_{L^1(\mathbb{R})} = 1$. Then let $\varrho_h(x) := \int_0^x \omega_h(\xi) \, d\xi$ and take $\Phi(t) := \varrho_h(t - t_1) - \varrho_h(t - t_2)$,

where $0 \leqslant t_1 < t_2 \leqslant T$. Taking $h \to 0$, we obtain

$$\int_{\mathbb{R}} |u(\cdot, t_2) - v(\cdot, t_2)| \, dx - \int_{\mathbb{R}} |u(\cdot, t_1) - v(\cdot, t_1)| \, dx \leqslant E,$$

$$E := \int_{t_1}^{t_2} \Big\{ \mathrm{sgn}(v_+ - u_+) \big(\varphi(v_+) - \varphi(u_+) - \gamma_+(v_+ - u_+) \big)$$

$$- \mathrm{sgn}(v_- - u_-) \big(\varphi(v_-) - \varphi(u_-) \big) \Big\} dt. \qquad (3.3.17)$$

To prove the L^1 contraction property, we verify that $E \leqslant 0$ by showing that the jump conditions ensure that the integrand in (3.3.17) is non-positive for almost all $t \in (0, T)$. To this end, we give a name to this integrand:

$$S := \mathrm{sgn}(v_+ - u_+) \big(\varphi(v_+) - \gamma_+ v_+ - \varphi(u_+) + \gamma_+ u_+ \big)$$

$$- \mathrm{sgn}(v_- - u_-) \big(\varphi(v_-) - \varphi(u_-) \big).$$

Our goal now is to show that $S \leqslant 0$. We prove this by examining the cases corresponding to the ordering among the four numbers u_-, u_+, v_-, v_+. There are 24 such cases, but we can eliminate half of them, since interchanging u_- with v_- and u_+ with v_+ leads to the same proofs, only with different labels.

Case 1. $u_- \leqslant v_- \leqslant u_+ \leqslant v_+$. In this case

$$S = \varphi(v_+) - \gamma_+ v_+ - \varphi(u_+) + \gamma_+ u_+ - \big(\varphi(v_-) - \varphi(u_-) \big).$$

Taking $c = v_-$ in (3.3.4), we get

$$\varphi(u_-) - \varphi(v_-) \leqslant 0.$$

Interchanging u and v and setting $c = u_+$ in (3.3.3), we obtain $\varphi(v_+) - \varphi(u_+) - \gamma_+(v_+ - u_+) \leqslant 0$, which makes it clear that $S \leqslant 0$.

Case 2. $u_- \leqslant v_- \leqslant v_+ \leqslant u_+$. In this case

$$S = \varphi(u_+) - \gamma_+ u_+ - \varphi(v_+) + \gamma_+ v_+ - \big(\varphi(v_-) - \varphi(u_-) \big)$$

$$\leqslant \varphi(u_+) - \gamma_+ u_+ - \varphi(v_+) + \gamma_+ v_+.$$

Here we have used that $\varphi(v_-) - \varphi(u_-) \geqslant 0$, which results by taking $c = v_-$ in (3.3.4). Now letting $c = v_+$ in (3.3.3), we get $\varphi(u_+) - \varphi(v_+) \leqslant \gamma_+(u_+ - v_+)$, which implies $S \leqslant 0$.

Case 3. $u_- \leqslant u_+ \leqslant v_- \leqslant v_+$. In this case

$$S = \varphi(v_+) - \gamma_+ v_+ - \varphi(u_+) + \gamma_+ u_+ - \big(\varphi(v_-) - \varphi(u_-) \big).$$

From (3.3.9), $\varphi(u_-) - \varphi(u_+) \leqslant 0$, and so

$$S \leqslant \varphi(v_+) - \varphi(v_-) - \gamma_+(v_+ - u_+) \leqslant \varphi(v_+) - \varphi(v_-) - \gamma_+(v_+ - v_-).$$

Taking $c = v_-$ in (3.3.3), it is now clear that $S \leqslant 0$.

Case 4. $u_- \leqslant u_+ \leqslant v_+ \leqslant v_-$. In this case

$$S = \varphi(v_+) - \gamma_+ v_+ - \varphi(u_+) + \gamma_+ u_+ - \big(\varphi(v_-) - \varphi(u_-)\big).$$

From (3.3.9), $\varphi(u_-) - \varphi(u_+) \leqslant 0$, $\varphi(v_+) - \varphi(v_-) \leqslant 0$ and so

$$S \leqslant -\gamma_+(v_+ - u_+) \leqslant 0.$$

Case 5. $u_- \leqslant v_+ \leqslant v_- \leqslant u_+$. In this case

$$S = \varphi(u_+) - \gamma_+ u_+ - \varphi(v_+) + \gamma_+ v_+ - \big(\varphi(v_-) - \varphi(u_-)\big).$$

Taking $c = v_+$ in (3.3.3), and then $c = v_-$ in (3.3.4), we find that

$$\varphi(u_+) - \varphi(v_+) - \gamma_+(u_+ - v_+) \leqslant 0, \quad \varphi(v_-) - \varphi(u_-) \geqslant 0,$$

which clearly yields $S \leqslant 0$.

Case 6. $u_- \leqslant v_+ \leqslant u_+ \leqslant v_-$. In this case

$$S = \varphi(u_+) - \gamma_+ u_+ - \varphi(v_+) + \gamma_+ v_+ - \big(\varphi(v_-) - \varphi(u_-)\big).$$

Letting $c = v_+$ in (3.3.3) results in

$$\varphi(u_+) - \varphi(v_+) \leqslant \gamma_+(u_+ - v_+),$$

and so

$$S \leqslant -\big(\varphi(v_-) - \varphi(u_-)\big).$$

Taking $c = v_+$ in (3.3.4) gives $\varphi(v_+) - \varphi(u_-) \geqslant 0$. Also, from (3.3.9), we see that $\varphi(v_-) \geqslant \varphi(v_+)$. Combining these inequalities gives $\varphi(v_-) - \varphi(u_-) \geqslant 0$, and thus $S \leqslant 0$.

Case 7. $u_+ \leqslant u_- \leqslant v_- \leqslant v_+$. In this case

$$\begin{aligned}
S &= \varphi(v_+) - \gamma_+ v_+ - \varphi(u_+) + \gamma_+ u_+ - \big(\varphi(v_-) - \varphi(u_-)\big) \\
&\leqslant \varphi(v_+) - \gamma_+ v_+ - \varphi(u_+) + \gamma_+ u_+ - \big(\varphi(v_-) - \varphi(u_-)\big) + \gamma_+ v_- - \gamma_+ u_- \\
&= \varphi(v_+) - \varphi(v_-) - \gamma_+(v_+ - v_-) - \big(\varphi(u_+) - \varphi(u_-) - \gamma_+(u_+ - u_-)\big).
\end{aligned}$$

By (3.3.9), we have the inequalities

$$\varphi(v_+) - \varphi(v_-) - \gamma_+(v_+ - v_-) \leqslant 0, \quad \varphi(u_+) - \varphi(u_-) - \gamma_+(u_+ - u_-) \geqslant 0,$$

yielding $S \leqslant 0$.

Case 8. $u_+ \leqslant u_- \leqslant v_+ \leqslant v_-$. In this case

$$S = \varphi(v_+) - \gamma_+ v_+ - \varphi(u_+) + \gamma_+ u_+ - \big(\varphi(v_-) - \varphi(u_-)\big).$$

By (3.3.9), $\varphi(v_+) \leqslant \varphi(v_-)$, which results in the inequality

$$S \leqslant \varphi(u_-) - \varphi(u_+) - \gamma_+(v_+ - u_+) \leqslant \varphi(u_-) - \varphi(u_+) - \gamma_+(u_- - u_+).$$

Taking $c = u_-$ in (3.3.5), we find that $\varphi(u_-) - \varphi(u_+) - \gamma_+(u_- - u_+) \leqslant 0$, yielding $S \leqslant 0$.

Case 9. $v_+ \leqslant u_- \leqslant v_- \leqslant u_+$. In this case

$$S = \varphi(u_+) - \gamma_+ u_+ - \varphi(v_+) + \gamma_+ v_+ - \big(\varphi(v_-) - \varphi(u_-)\big).$$

Taking $c = u_-$ in (3.3.5) gives $\varphi(v_+) - \varphi(u_-) \geqslant \gamma_+(v_+ - u_-)$, which we can rearrange as $-\varphi(v_+) + \varphi(u_-) + \gamma_+ v_+ \leqslant \gamma_+ u_-$. From this it follows that

$$S \leqslant \varphi(u_+) - \varphi(v_-) - \gamma_+ u_+ + \gamma_+ u_-.$$

Now (3.3.10) tells us that $v_+ \leqslant v_- \leqslant u^*$. Recalling that $u \mapsto \varphi(u)$ is non-decreasing on $[0, u^*]$, and that $v_+ \leqslant u_- \leqslant v_-$, we find that $\varphi(u_-) \leqslant \varphi(v_-)$, and so

$$S \leqslant \varphi(u_+) - \varphi(u_-) - \gamma_+ u_+ + \gamma_+ u_-.$$

The right side of this last inequality is non-positive due to (3.3.9), and so $S \leqslant 0$.

Case 10. $v_+ \leqslant u_- \leqslant u_+ \leqslant v_-$. In this case

$$S = \varphi(u_+) - \gamma_+ u_+ - \varphi(v_+) + \gamma_+ v_+ - \big(\varphi(v_-) - \varphi(u_-)\big).$$

Taking $c = u_+$ in (3.3.5) gives $\varphi(v_+) - \varphi(u_+) \geqslant \gamma_+(v_+ - u_+)$, from which we derive $S \leqslant \varphi(u_-) - \varphi(v_-)$. From (3.3.10) we have that $v_+ \leqslant v_- \leqslant u^*$. Since also $u_- \leqslant v_- \leqslant u^*$, we see that $\varphi(u_-) \leqslant \varphi(v_-)$, yielding $S \leqslant 0$.

Case 11. $u_+ \leqslant v_- \leqslant u_- \leqslant v_+$. In this case

$$S = \varphi(v_+) - \gamma_+ v_+ - \varphi(u_+) + \gamma_+ u_+ - \big(\varphi(u_-) - \varphi(v_-)\big).$$

Taking $c = u_-$ in (3.3.3) results in

$$\varphi(v_+) - \varphi(u_-) - \gamma_+ v_+ \leqslant -\gamma_+ u_-,$$

which in turn gives us

$$S \leqslant -\varphi(u_+) + \gamma_+ u_+ + \varphi(v_-) - \gamma_+ u_-.$$

From (3.3.10) we have that $u_+ \leqslant u_- \leqslant u^*$. Since also $v_- \leqslant u_- \leqslant u^*$, we have $\varphi(v_-) \leqslant \varphi(u_-)$, and so

$$S \leqslant -\varphi(u_+) + \gamma_+ u_+ + \varphi(u_-) - \gamma_+ u_- = \varphi(u_-) - \varphi(u_+) - \gamma_+(u_- - u_+).$$

This last quantity is non-positive, due to (3.3.9), resulting in $S \leqslant 0$.

Case 12. $u_+ \leqslant v_+ \leqslant u_- \leqslant v_-$. In this case

$$S = \varphi(v_+) - \gamma_+ v_+ - \varphi(u_+) + \gamma_+ u_+ - \big(\varphi(v_-) - \varphi(u_-)\big).$$

Taking $c = v_+$ in (3.3.5) results in

$$\varphi(v_+) - \varphi(u_+) - \gamma_+(v_+ - u_+) \leqslant 0,$$

which in turn gives us $S \leqslant \varphi(u_-) - \varphi(v_-)$. From (3.3.10) we have that $v_+ \leqslant v_- \leqslant u^*$. Since also $u_- \leqslant v_- \leqslant u^*$, we have $\varphi(u_-) \leqslant \varphi(v_-)$, making it clear that $S \leqslant 0$. $\qquad\square$

4 Numerical scheme and some properties

In this section we discuss a difference scheme that applies to the full model (1.1.1). We begin the definition of the algorithm by discretizing the spatial domain $\mathbb{R}$ into cells $I_j := [x_{j-1/2}, x_{j+1/2})$, $j \in \mathbb{Z}$, where $x_k = k\Delta x$ for $k = 0, \pm 1/2, \pm 1, \pm 3/2, \ldots$. Similarly, the time interval $(0, T)$ is discretized via $t_n = n\Delta t$ for $n = 0, \ldots, N$, where $N = \lfloor T/\Delta t \rfloor + 1$, which results in the time strips $I^n := [t_n, t_{n+1})$, $n = 0, \ldots, N-1$. Here $\Delta x > 0$ and $\Delta t > 0$ denote the spatial and temporal discretization parameters, respectively. These parameters are chosen so that the following CFL condition holds:

$$\lambda \max_{u \in [0,1], x \in \mathbb{R}} |f_u(\gamma(x), u)| + \lambda \max_{x \in \mathbb{R}} \gamma^3(x) \leqslant \frac{1}{2}, \qquad \lambda := \frac{\Delta t}{\Delta x}. \tag{4.4.1}$$

When sending $\Delta \downarrow 0$ we will do so with the ratio λ kept constant. We use the symbol Δ to refer to the discretization parameters collectively: $\Delta = (\Delta x, \Delta t)$.

We propose a scheme that is a direct modification of the one described in [12]. Let U_j^n denote our approximation to $u(x_j, t^n)$. Then the marching formula for our new scheme is

$$U_j^{n+1} = U_j^n - \lambda \Delta_- h(\gamma_{j+1/2}, U_{j+1}^n, U_j^n) + \lambda \gamma_j^3 \Delta_+ U_j^n. \tag{4.4.2}$$

Here $\gamma_{j+1/2} = \gamma(x_{j+1/2}-)$, and $\gamma_j^3 := \gamma^3(x_j-)$. In (4.4.2) the symbols $\Delta_\pm$ are spatial difference operators:

$$\Delta_- h(\gamma_{j+1/2}, U_{j+1}^n, U_j^n) = h(\gamma_{j+1/2}, U_{j+1}^n, U_j^n) - h(\gamma_{j-1/2}, U_j^n, U_{j-1}^n),$$

and $\Delta_+ U_j^n = U_{j+1}^n - U_j^n$.

The main difference between (4.4.2) and the scheme defined in [12] is the new term $\lambda \gamma_j^3 \Delta_+ U_j^n$ that incorporates the sink feature. The use of the forward difference Δ_+ in this new sink term is deliberate; we bias this difference to preserve the upwind nature of the scheme. Here we are explicitly using the assumption that $\gamma^3(x) \geqslant 0$. The function $h(\gamma, v, u)$ is the Engquist-Osher (EO henceforth) numerical flux [26]

$$h(\gamma, v, u) := \frac{1}{2}\big(f(\gamma, u) + f(\gamma, v)\big) - \frac{1}{2} \int_u^v |f_u(\gamma, w)| \, dw. \tag{4.4.3}$$

To define an approximate solution not just at the mesh points, but on all of Π_T, we let χ_j^n denote the indicator for the rectangle $I_j \times I^n$ and introduce

$$u^\Delta(x, t) := \sum_{n=0}^N \sum_{j \in \mathbb{Z}} \chi_j^n(x, t) U_j^n.$$

Although the scheme is not conservative, several important properties of monotonicity are preserved. The following lemma is adapted from Lemma 3.1 of Bürger *et al.* [12].

Lemma 4.1 *The computed solution U_j^n belongs to the interval $[0, 1]$. Moreover, the difference scheme* (4.4.2) *is monotone.*

Proof We start by noting that the marching formula (4.4.2) defines U_j^{n+1} as a function of the three independent variables U_{j-1}^n, U_j^n, U_{j+1}^n Using (4.4.2), we compute the partial derivatives of U_j^{n+1} with respect to these variables:

$$\frac{\partial U_j^{n+1}}{\partial U_{j+1}^n} = -\lambda f_u^- \big(\gamma_{j+1/2}, U_{j+1}^n\big) + \lambda \gamma_j^3 \geqslant 0, \quad \frac{\partial U_j^{n+1}}{\partial U_{j-1}^n} = \lambda f_u^+ \big(\gamma_{j-1/2}, U_{j-1}^n\big) \geqslant 0,$$

$$\frac{\partial U_j^{n+1}}{\partial U_j^n} = 1 + \lambda f_u^- \big(\gamma_{j-1/2}, U_j^n\big) - \lambda f_u^+ \big(\gamma_{j+1/2}, U_j^n\big) - \lambda \gamma_j^3.$$

Thus, U_j^{n+1} is a non-decreasing function of the conserved variables at t_n if

$$1 + \lambda f_u^- \big(\gamma_{j-1/2}, U_j^n\big) - \lambda f_u^+ \big(\gamma_{j+1/2}, U_j^n\big) - \lambda \gamma_j^3 \geqslant 0.$$

This will hold if $U_j^n \in [0, 1]$ for all j and the CFL condition (4.4.1) is satisfied. The rest of the proof is similar to the proof of Lemma 3.1 of [12], and is omitted. □

Next we establish a fundamental time-continuity estimate.

Lemma 4.2 *There exists a constant C, independent of Δ and n, such that*

$$\Delta x \sum_{j \in \mathbb{Z}} |U_j^{n+1} - U_j^n| \leqslant \Delta x \sum_{j \in \mathbb{Z}} |U_j^1 - U_j^0| \leqslant C \Delta t. \tag{4.4.4}$$

Proof Starting from the marching formula (4.4.2), we can express the time differences as follows:

$$
\begin{aligned}
U_j^{n+1} - U_j^n &= U_j^n - U_j^{n-1} - \lambda \Delta_- \big[h\big(\gamma_{j+1/2}, U_{j+1}^n, U_j^n\big) - h\big(\gamma_{j+1/2}, U_{j+1}^{n-1}, U_j^{n-1}\big) \big] \\
&\quad + \lambda \gamma_j^3 \Delta_+ U_j^n - \lambda \gamma_j^3 \Delta_+ U_j^{n-1} \\
&= \big(1 - \lambda C_{j+1/2}^{n-1/2} + \lambda B_{j-1/2}^{n-1/2} - \lambda \gamma_j^3\big)\big(U_j^n - U_j^{n-1}\big) \\
&\quad - \lambda B_{j+1/2}^{n-1/2}\big(U_{j+1}^n - U_{j+1}^{n-1}\big) + \lambda C_{j-1/2}^{n-1/2}\big(U_{j-1}^n - U_{j-1}^{n-1}\big) \\
&\quad + \lambda \gamma_j^3\big(U_{j+1}^n - U_{j+1}^{n-1}\big),
\end{aligned}
$$

where we define

$$B_{j+1/2}^{n-1/2} := \int_0^1 f_u^- \big(\gamma_{j+1/2}, \theta U_{j+1}^n + (1-\theta)U_{j+1}^{n-1}\big)\, d\theta \leqslant 0,$$

$$C_{j+1/2}^{n-1/2} := \int_0^1 f_u^+ \big(\gamma_{j+1/2}, \theta U_j^n + (1-\theta)U_j^{n-1}\big)\, d\theta \geqslant 0.$$

Due to the CFL condition (4.4.1),

$$1 - \lambda C_{j+1/2}^{n-1/2} + \lambda B_{j-1/2}^{n-1/2} - \lambda \gamma_j^3 \geqslant 0.$$

Thus, we conclude that

$$
\begin{aligned}
|U_j^{n+1} - U_j^n| &\leqslant \left(1 - \lambda C_{j+1/2}^{n-1/2} + \lambda B_{j-1/2}^{n-1/2} - \lambda \gamma_j^3\right)|U_j^n - U_j^{n-1}| \\
&\quad - \lambda B_{j+1/2}^{n-1/2}|U_{j+1}^n - U_{j+1}^{n-1}| + \lambda C_{j-1/2}^{n-1/2}|U_{j-1}^n - U_{j-1}^{n-1}| \\
&\quad + \lambda \gamma_j^3|U_{j+1}^n - U_{j+1}^{n-1}| \\
&\leqslant \left(1 - \lambda C_{j+1/2}^{n-1/2} + \lambda B_{j-1/2}^{n-1/2} - \lambda \gamma_j^3\right)|U_j^n - U_j^{n-1}| \\
&\quad - \lambda B_{j+1/2}^{n-1/2}|U_{j+1}^n - U_{j+1}^{n-1}| + \lambda C_{j-1/2}^{n-1/2}|U_{j-1}^n - U_{j-1}^{n-1}| \\
&\quad + \lambda \gamma_{j+1}^3|U_{j+1}^n - U_{j+1}^{n-1}|.
\end{aligned}
$$

Here we have used the fact that $x \mapsto \gamma^3(x)$ in non-decreasing when replacing γ_j^3 by γ_{j+1}^3. Summing this inequality over j and multiplying by Δx gives

$$\Delta x \sum_{j \in \mathbb{Z}} |U_j^{n+1} - U_j^n| \leqslant \Delta x \sum_{j \in \mathbb{Z}} |U_j^n - U_j^{n-1}|.$$

Applying this last inequality inductively, we arrive at

$$\Delta x \sum_{j \in \mathbb{Z}} |U_j^{n+1} - U_j^n| \leqslant \Delta x \sum_{j \in \mathbb{Z}} |U_j^1 - U_j^0|.$$

The rest of the proof is similar to the proof of Lemma 3.2 of [12] and is omitted. $\square$

Lemmas 4.1 and 4.2 provide several important stability properties of our new difference scheme. We will not pursue the analysis for the full model (1.1.1), but focus on the reduced problem described in Section 2.4.

5 Convergence to an entropy solution for the reduced problem

We can write the scheme for the reduced problem (1.1.2) as

$$U_j^{n+1} = U_j^n - \lambda \Delta_- h\left(U_{j+1}^n, U_j^n\right) + \lambda \gamma_j \Delta_+ U_j^n. \tag{5.5.1}$$

Here we are abusing the notation slightly by continuing to use the symbol h of §4 for the numerical flux, i.e.

$$h(v, u) = \frac{1}{2}\left(\varphi(v) + \varphi(u)\right) - \frac{1}{2}\int_u^v |\varphi'(w)|\, dw.$$

The appropriate CFL condition for our reduced problem is

$$\lambda \max_{u \in [0,1], x \in \mathbb{R}} |\varphi'(u)| + \lambda \max_{x \in \mathbb{R}} \gamma(x) \leqslant \frac{1}{2}, \qquad \lambda := \frac{\Delta t}{\Delta x}. \tag{5.5.2}$$

Lemmas 4.1 and 4.2 remain valid in this setting, and need not be repeated. In order to establish compactness, we will also need a spatial variation bound, which is provided by the following lemma. Let $TV(z)$ denote the total variation of a function $z \in L^1_{\mathrm{loc}}(\mathbb{R})$.

Lemma 5.1 *For any $t \in [0, T]$ we have the spatial variation bound*

$$TV(u^\Delta(\cdot, t)) \leqslant C, \tag{5.5.3}$$

where C is independent of Δ and t for $t \in [0, T]$.

Proof We start by writing the scheme (5.5.1) in incremental form

$$U_j^{n+1} = U_j^n + C_{j+1/2}^n \Delta_+ U_j^n - D_{j-1/2}^n \Delta_- U_j^n,$$

where

$$C_{j+1/2}^n = \lambda\left(\frac{\varphi(U_j^n) - h(U_{j+1}^n, U_j^n)}{\Delta_+ U_j^n} + \gamma_j \right), \quad D_{j-1/2}^n = \lambda \frac{\varphi(U_j^n) - h(U_j^n, U_{j-1}^n)}{\Delta_- U_j^n}.$$

Using the monotonicity of the numerical flux h, that $\gamma_j \geqslant 0$, and the CFL condition (5.5.2), one can easily check that

$$C_{j+1/2}^n \geqslant 0, \quad D_{j+1/2}^n \geqslant 0, \quad C_{j+1/2}^n + D_{j+1/2}^n \leqslant 1.$$

It now follows from Harten's lemma (Lemma 2.2 of [32]) that

$$\sum_{j \in \mathbb{Z}} |U_{j+1}^{n+1} - U_j^{n+1}| \leqslant \sum_{j \in \mathbb{Z}} |U_{j+1}^n - U_j^n|.$$

Continuing by induction, we conclude that

$$TV(u^\Delta(\cdot, t)) \leqslant TV(u^\Delta(\cdot, 0)) \leqslant TV(u_0),$$

and the proof is complete.   □

In what follows, we will employ the following regularizations of the function $\gamma(x)$.

$$\overline{\gamma}^\epsilon(x) := \begin{cases} 0 & \text{for } x \leqslant -\epsilon, \\ ((x+\epsilon)/\epsilon)\gamma_+ & \text{for } -\epsilon \leqslant x \leqslant 0, \\ \gamma_+ & \text{for } x \geqslant 0, \end{cases}$$

$$\underline{\gamma}^\epsilon(x) := \begin{cases} 0 & \text{for } x \leqslant 0, \\ (x/\epsilon)\gamma_+ & \text{for } 0 \leqslant x \leqslant \epsilon, \\ \gamma_+ & \text{for } x \geqslant \epsilon. \end{cases}$$

Observe that $\underline{\gamma}^\epsilon(x) \leqslant \gamma(x) \leqslant \overline{\gamma}^\epsilon(x)$ for all $x \in \mathbb{R}$. When discretizing $\underline{\gamma}^\epsilon$ and $\overline{\gamma}^\epsilon$, we do so in the same manner as γ, thus preserving the ordering $\underline{\gamma}_j^\epsilon \leqslant \gamma_j \leqslant \overline{\gamma}_j^\epsilon$.

One more preliminary issue before we discuss entropy conditions is the existence of traces along the line $x = 0$, $t \in [0, T]$. Our spatial BV bounds carry over to the limit solution u, guaranteeing that we have limits from both the left and right, denoted $u_-(t), u_+(t)$ or simply u_-, u_+, for a.e. $t \in [0, T]$.

Lemma 5.2 *Any (subsequential) limit u of the scheme* (5.5.1) *satisfies the entropy conditions* (3.3.1)–(3.3.6).

Proof The proof of the Kružkov-type entropy inequalities (3.3.1), (3.3.2) is standard [18], and is omitted.

We now turn to the proof of (3.3.3). The following discrete entropy inequality holds for any $c \in \mathbb{R}$; this follows from the monotonicity of the scheme:

$$U_j^{n+1} \vee c \leqslant U_j^n \vee c - \lambda \Delta_+ h \left(U_j^n \vee c, U_{j-1}^n \vee c \right) + \lambda \gamma_j \Delta_+ \left(U_j^n \vee c \right). \qquad (5.5.4)$$

Now let

$$V_j^n := \begin{cases} c & \text{for } j \leqslant 0, \\ U_j^n \vee c & \text{for } j > 0, \end{cases} \qquad v(x, t) := \begin{cases} c & \text{for } x < 0, \\ u(x, t) \vee c & \text{for } x > 0. \end{cases}$$

Note that

$$\Delta_+ V_0^n = U_1^n \vee c - c \geqslant 0. \qquad (5.5.5)$$

Since $\gamma_j = 0$ for $j \leqslant 0$, and $\Delta_+ V_j^n = \Delta_+(U_j^n \vee c)$ for $j > 0$, we can replace inequality (5.5.4) by

$$U_j^{n+1} \vee c \leqslant U_j^n \vee c - \lambda \Delta_+ h \left(U_j^n \vee c, U_{j-1}^n \vee c \right) + \lambda \gamma_j \Delta_+ V_j^n. \qquad (5.5.6)$$

Since $\overline{\gamma}_j^\epsilon \geqslant \gamma_j = 0$ for $j \leqslant 0$ and $\overline{\gamma}_j^\epsilon = \gamma_j = \gamma_+$ for $j > 0$, in view of (5.5.5) we can replace inequality (5.5.6) by

$$U_j^{n+1} \vee c \leqslant U_j^n \vee c - \lambda \Delta_+ h \left(U_j^n \vee c, U_{j-1}^n \vee c \right) + \lambda \overline{\gamma}_j^\epsilon \Delta_+ V_j^n. \qquad (5.5.7)$$

Employing the identity

$$A_j \Delta_+ B_j = \Delta_+ \left(A_j B_j \right) - B_{j+1} \Delta_+ A_j, \qquad (5.5.8)$$

we can rewrite (5.5.7) in the form

$$U_j^{n+1} \vee c \leqslant U_j^n \vee c - \lambda \Delta_+ \left(h \left(U_j^n \vee c, U_{j-1}^n \vee c \right) - \overline{\gamma}_j^\epsilon V_j^n \right) - \lambda V_{j+1}^n \Delta_+ \overline{\gamma}_j^\epsilon. \qquad (5.5.9)$$

Let $0 \leqslant \psi \in \mathscr{D}(\Pi_T)$, and $\psi_j^n = \psi(x_j, t^n)$. Proceeding as in the proof of the Lax-Wendroff theorem, we move all terms in (5.5.9) to the left-hand side of the inequality, multiply by

$\psi_j^n \Delta x$, and sum over $j \in \mathbb{Z}$, $n \geqslant 0$, and finally sum by parts to get

$$\Delta x \Delta t \sum_{j \in \mathbb{Z}} \sum_{n \geqslant 0} \left(U_j^n \vee c \right) \frac{\psi_j^{n+1} - \psi_j^n}{\Delta t}$$

$$+ \Delta x \Delta t \sum_{j \in \mathbb{Z}} \sum_{n \geqslant 0} \left[h \left(U_j^n \vee c, U_{j-1}^n \vee c \right) - \overline{\gamma}_j^\epsilon V_j^n \right] \frac{\Delta_+ \psi_j^n}{\Delta x} \qquad (5.5.10)$$

$$- \Delta x \Delta t \sum_{j \in \mathbb{Z}} \sum_{n \geqslant 0} \frac{\Delta_+ \overline{\gamma}_j^\epsilon}{\Delta x} V_{j+1}^n \psi_j^n \geqslant 0.$$

When $\Delta \downarrow 0$, the bounded convergence theorem yields

$$\iint_{\Pi_T} \left((u \vee c)\psi_t + (\varphi(u \vee c) - \overline{\gamma}^\epsilon(x)v)\psi_x \right) dx\, dt - \iint_{\Pi_T} (\overline{\gamma}^\epsilon)'(x)\, v\, \psi\, dx\, dt \geqslant 0. \quad (5.5.11)$$

With the observation that

$$(\overline{\gamma}^\epsilon)'(x) = \begin{cases} \gamma_+/\epsilon & \text{for } x \in (-\epsilon, 0), \\ 0 & \text{for } x \notin (-\epsilon, 0), \end{cases}$$

when $\epsilon \downarrow 0$ we obtain

$$\iint_{\Pi_T} (\overline{\gamma}^\epsilon)'(x)\, v\, \psi\, dx\, dt \to \gamma_+ c \int_0^T \psi(0, t)\, dt.$$

Combining this with an application of the bounded convergence theorem, when $\epsilon \downarrow 0$, (5.5.11) yields the inequality

$$\iint_{\Pi_T} \left((u \vee c)\psi_t + (\varphi(u \vee c) - \gamma(x)v)\psi_x \right) dx\, dt - \gamma_+ c \int_0^T \psi(0, t)\, dt \geqslant 0. \qquad (5.5.12)$$

By applying a standard test function argument to (5.5.12), we find that for a.e. $t \in (0, T)$,

$$\varphi(u_-(t) \vee c) - \gamma_- c - \left(\varphi(u_+(t) \vee c) - \gamma_+(u_+(t) \vee c) \right) - \gamma_+ c \geqslant 0.$$

Recalling that $\gamma_- = 0$, $u_- \leqslant c \leqslant u_+$, dropping the dependence on t, and rearranging, this inequality becomes

$$\varphi(u_+) - \varphi(c) \leqslant \gamma_+(u_+ - c),$$

and the proof of (3.3.3) is complete.

For the proof of (3.3.4) we use the monotonicity of the scheme to derive the discrete entropy inequality

$$U_j^{n+1} \wedge c \geqslant U_j^n \wedge c - \lambda \Delta_+ h \left(U_j^n \wedge c, U_{j-1}^n \wedge c \right) + \lambda \gamma_j \Delta_+ \left(U_j^n \wedge c \right). \qquad (5.5.13)$$

Let

$$W_j^n := \begin{cases} c & \text{for } j \leqslant 0, \\ U_j^n \wedge c & \text{for } j > 0, \end{cases}, \qquad w(x, t) := \begin{cases} c & \text{for } x < 0, \\ u(x, t) \wedge c & \text{for } x > 0. \end{cases}$$

Observing that

$$\Delta_+(U_0^n \wedge c) = U_1^n \wedge c - U_0^n \wedge c \geqslant \Delta_+ W_0^n = U_1^n \wedge c - c \leqslant 0,$$

we find that the following inequality holds:

$$U_j^{n+1} \wedge c \geqslant U_j^n \wedge c - \lambda \Delta_+ h\left(U_j^n \wedge c, U_{j-1}^n \wedge c\right) + \lambda \gamma_j \Delta_+ W_j^n.$$

Using $0 \leqslant \gamma_j \leqslant \overline{\gamma}_j^\epsilon$ and $\Delta_+ W_0^n \leqslant 0$, we also have

$$U_j^{n+1} \wedge c \geqslant U_j^n \wedge c - \lambda \Delta_+ h\left(U_j^n \wedge c, U_{j-1}^n \wedge c\right) + \lambda \overline{\gamma}_j^\epsilon \Delta_+ W_j^n.$$

Proceeding as in the proof of (3.3.3), we find that

$$\iint_{\Pi_T} \left((u \wedge c)\psi_t + \left(\varphi(u \wedge c) - \overline{\gamma}^\epsilon(x)w\right)\psi_x\right) dx\, dt - \iint_{\Pi_T} (\overline{\gamma}^\epsilon)'(x)\, w\, \psi\, dx\, dt \leqslant 0,$$

from which it follows that

$$\varphi(u_-(t) \wedge c) - \gamma_- c - \left(\varphi(u_+(t) \wedge c) - \gamma_+(u_+(t) \wedge c)\right) - \gamma_+ c \leqslant 0,$$

and this holds for a.e. $t \in [0, T]$. Recalling that $\gamma_- = 0$, and then observing that the terms involving $\gamma_+(u_+(t) \wedge c)$ and $\gamma_+ c$ cancel, the proof of (3.3.4) is complete.

For the proof of (3.3.6), we start from the discrete entropy inequality (5.5.4), and then apply the identity (5.5.8) to get

$$\begin{aligned}
U_j^{n+1} \vee c &\leqslant U_j^n \vee c - \lambda \Delta_+ \left(h\left(U_j^n \vee c, U_{j-1}^n \vee c\right) - \gamma_j(U_j^n \vee c)\right) \\
&\quad - \lambda(U_{j+1}^n \vee c)\Delta_+ \gamma_j.
\end{aligned} \tag{5.5.14}$$

We then define

$$\tilde{V}_j^n := \begin{cases} U_j^n \vee c & \text{for } j \leqslant 0, \\ c & \text{for } j > 0, \end{cases} \qquad \tilde{v}(x,t) := \begin{cases} u(x,t) \vee c & \text{for } x < 0, \\ c & \text{for } x > 0, \end{cases}$$

and observe that it is possible to replace the inequality (5.5.14) by

$$U_j^{n+1} \vee c \leqslant U_j^n \vee c - \lambda \Delta_+ \left(h\left(U_j^n \vee c, U_{j-1}^n \vee c\right) - \gamma_j(U_j^n \vee c)\right) - \lambda \tilde{V}_{j+1}^n \Delta_+ \gamma_j.$$

More specifically, this inequality holds because $\Delta_+ \gamma_j = 0$, except at $j = 0$, and $U_1^n \vee c \geqslant \tilde{V}_1 = c$. Another application of the identity (5.5.8) yields

$$\begin{aligned}
U_j^{n+1} \vee c &\leqslant U_j^n \vee c - \lambda \Delta_+ \left(h\left(U_j^n \vee c, U_{j-1}^n \vee c\right) - \gamma_j(U_j^n \vee c) + \gamma_j \tilde{V}_j^n\right) \\
&\quad + \lambda \gamma_j \Delta_+ \tilde{V}_j^n.
\end{aligned} \tag{5.5.15}$$

Since $\Delta_+ \tilde{V}_j^n = 0$ for $j > 0$, $\Delta_+ \tilde{V}_0^n \leqslant 0$, $\underline{\gamma}_j^\epsilon = \gamma_j$ for $j < 0$, and $\underline{\gamma}_j^\epsilon \leqslant \gamma_j$ for $j \geqslant 0$, we can

replace (5.5.15) by

$$U_j^{n+1} \vee c \leqslant U_j^n \vee c - \lambda \Delta_+ \big(h \left(U_j^n \vee c, U_{j-1}^n \vee c \right) - \gamma_j (U_j^n \vee c) + \gamma_j \tilde{V}_j^n \big)$$
$$+ \lambda \underline{\gamma}_j^\epsilon \Delta_+ \tilde{V}_j^n.$$

A final application of (5.5.8) results in

$$U_j^{n+1} \vee c \leqslant U_j^n \vee c - \lambda \Delta_+ \big(h \left(U_j^n \vee c, U_{j-1}^n \vee c \right) - \gamma_j (U_j^n \vee c) + (\gamma_j - \underline{\gamma}_j^\epsilon) \tilde{V}_j^n \big)$$
$$- \lambda \tilde{V}_{j+1}^n \Delta_+ \underline{\gamma}_j^\epsilon.$$

The rest of the proof of (3.3.6) is similar to the proofs of (3.3.3) and (3.3.4), and so we omit the details.

The proof of (3.3.5) is similar to that of (3.3.6), the main difference being that one starts from the discrete entropy inequality (5.5.13) and uses the modified functions

$$\tilde{W}_j^n := \begin{cases} U_j^n \wedge c & \text{for } j \leqslant 0, \\ c & \text{for } j > 0, \end{cases} \qquad \tilde{w}(x,t) := \begin{cases} u(x,t) \wedge c & \text{for } x < 0, \\ c & \text{for } x > 0. \end{cases}$$

We omit the details. $\qquad\square$

We can now state and prove our main theorem.

Theorem 5.1 *As $\Delta \downarrow 0$, the approximations u^Δ generated by the scheme (5.5.1) converge in $L^1(\Pi_T)$ and a.e. in Π_T to the unique entropy solution u of the initial value problem (1.1.2), (1.1.4), (1.1.5).*

Proof For the approximations u^Δ, we have an L^∞ bound (Lemma 4.1), a time continuity bound (Lemma 4.2), and a spatial variation bound (Lemma 5.1). In addition, it is a straightforward exercise using the time continuity bound provided by Lemma 4.2 to derive a bound for the approximations u^Δ in the $L^1(\Pi_T)$ norm. Moreover, these bounds are independent of Δ, for $(x,t) \in \Pi_T$. It follows from standard compactness arguments that there is a subsequential limit, converging in $L^1(\Pi_T)$, and a.e. in Π_T, which we will denote u. A proof of (3.3.7), i.e. that the initial values are assumed in the strong L^1 sense is standard and is thus omitted. The proof is completed with an application of our Lemma 5.2, which guarantees that the subsequential limit u is an entropy solution. By our uniqueness result (Theorem 3.1), the entire sequence converges to u. $\qquad\square$

Theorem 5.1 shows that there exists a unique entropy solution to the initial value problem (1.1.2), (1.1.4), (1.1.5), i.e. that this problem is well-posed.

6 Variants of the difference scheme

The scheme described herein for the full problem has the slight inconvenience that to evaluate the Engquist-Osher flux function, one has to determine the extrema of the

composite flux function $q(u - u_\mathrm{F}) + b(u)$ for $q \in \{q_\mathrm{L}, \tilde{q}_\mathrm{R}\}$ numerically. This can be avoided if we determine the Engquist-Osher flux function for the function $b(u)$ only, and discretize the linear portion $q(u - u_\mathrm{F})$ by a properly oriented upwind stencil. The resulting scheme, to which we shall refer as "Scheme 1", then reads

$$
\begin{aligned}
U_j^{n+1} = U_j^n &- \lambda \Delta_- h^1 \big(\gamma_{j+1/2}^1, U_{j+1}^n, U_j^n\big) \\
&- \lambda w \big(\gamma_{j-1/2}^2, \gamma_{j+1/2}^2, U_{j-1}^n, U_j^n, U_{j+1}^n\big) + \lambda \gamma_j^3 \Delta_+ U_j^n,
\end{aligned}
$$

where $\gamma^1, \gamma^2, \gamma^3$ are defined in (1.1.8) and (1.1.9), and the function h^1 is the EO flux applied to the function $\gamma^1 b(u)$, i.e.

$$
h^1(\gamma^1, v, u) = \frac{\gamma^1}{2} \left(b(u) + b(v) - \int_u^v |b'(s)| \, ds \right),
$$

and the function w arises from determining the EO flux for the linear term $\gamma^2(x)(u - u_\mathrm{F})$, followed by differencing with respect to x, i.e.

$$
w \big(\gamma_{j-1/2}^2, \gamma_{j+1/2}^2, U_{j-1}^n, U_j^n, U_{j+1}^n\big) := \Delta_- \tilde{h}\big(\gamma_{j+1/2}^2, U_{j+1}^n - u_\mathrm{F}, U_j - u_\mathrm{F}\big),
$$

where we define

$$
\tilde{h}(\gamma^2, v, u) := \frac{1}{2} \left(\gamma^2(u + v) - \int_u^v |\gamma^2| \, ds \right).
$$

This yields the upwind formula

$$
\begin{aligned}
&w \big(\gamma_{j-1/2}^2, \gamma_{j+1/2}^2, U_{j-1}^n, U_j^n, U_{j+1}^n\big) \\
&= \begin{cases}
\gamma_{j+1/2}^2 \big(U_j^n - u_\mathrm{F}\big) - \gamma_{j-1/2}^2 \big(U_{j-1}^n - u_\mathrm{F}\big) & \text{if } \gamma_{j-1/2}^2 \geq 0 \text{ and } \gamma_{j+1/2}^2 \geq 0, \\
\gamma_{j+1/2}^2 \big(U_{j+1}^n - u_\mathrm{F}\big) - \gamma_{j-1/2}^2 \big(U_j^n - u_\mathrm{F}\big) & \text{if } \gamma_{j-1/2}^2 < 0 \text{ and } \gamma_{j+1/2}^2 < 0, \\
\big(\gamma_{j+1/2}^2 - \gamma_{j-1/2}^2\big) \big(U_j^n - u_\mathrm{F}\big) & \text{if } \gamma_{j+1/2}^2 \geq 0 \text{ and } \gamma_{j-1/2}^2 < 0.
\end{cases}
\end{aligned}
$$

For easy reference, let us refer to the scheme (4.4.2), (4.4.3), which is analyzed in this paper, as "Scheme 2". Clearly, Scheme 1 emerges from Scheme 2 by applying a direct upwind linearization, and avoiding the EO formula, for as many terms as possible. As we shall see, the performance of Scheme 1 is much inferior to that of Scheme 2 in terms of numerical viscosity. On the other hand, this observation suggests that an even better scheme can possibly be produced if we replace Scheme 2 by a new scheme, called Scheme 3, if we avoid any explicit linear upwind differences at all, and express the numerical flux on all segments as one EO flux. Thus, the marching formula for Scheme 3 is

$$
U_j^{n+1} = \begin{cases}
U_j^n - \lambda \Delta_- h^3 \big(\tilde{\gamma}_{j+1/2}, \gamma_{j+1/2}^3, U_{j+1}^n, U_j^n\big) & \text{for } j > 0, \\
U_j^n - \lambda \Delta_- h^2 \big(\tilde{\gamma}_{j+1/2}, U_{j+1}^n, U_j^n\big) & \text{for } j \leq 0,
\end{cases}
$$

(a) Case 1   (b) Case 2
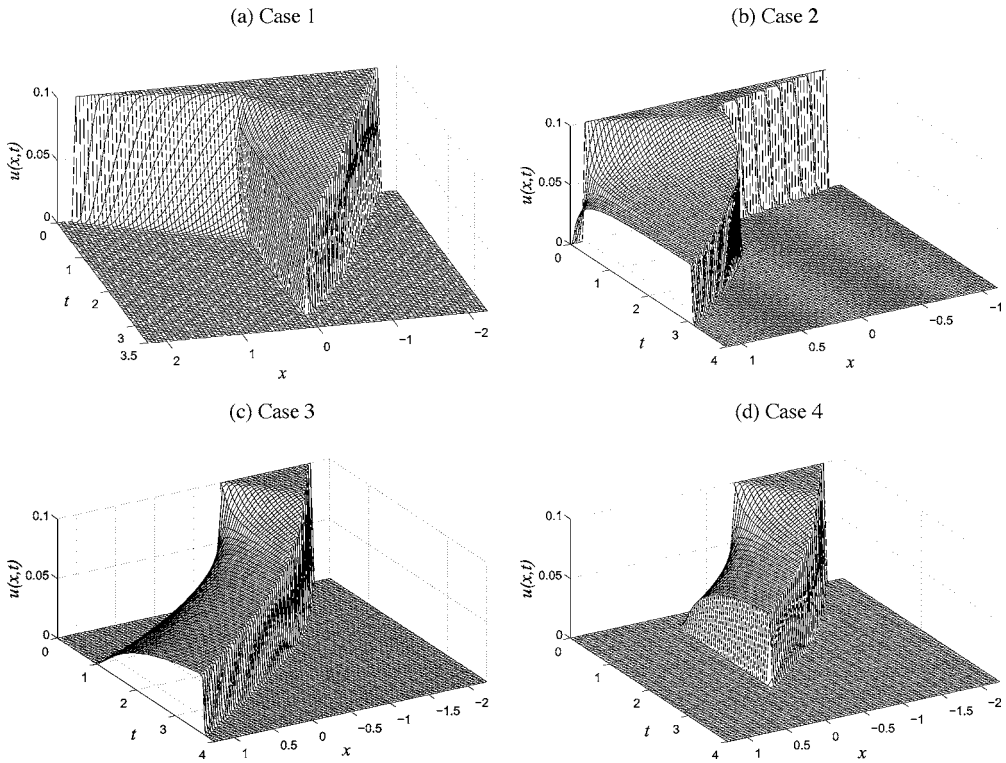

(c) Case 3   (d) Case 4

FIGURE 3. Numerical examples with $\Delta x = 0.0125$ for the reduced problem.

where we define $\tilde{\gamma} := (\gamma^1, \gamma^2)$ and

$$h^2(\tilde{\gamma}, v, u) := \frac{1}{2}\left(f(\tilde{\gamma}, u) + f(\tilde{\gamma}, v) - \int_u^v |f_u(\tilde{\gamma}, w)| \, dw\right),$$

$$h^3(\tilde{\gamma}, \gamma^3, v, u) := \frac{1}{2}\left(f(\tilde{\gamma}, u) + f(\tilde{\gamma}, v) - \gamma^3(u + v) - \int_u^v |f_u(\tilde{\gamma}, w) - \gamma^3| \, dw\right).$$

For the simplified version of Scheme 1 that applies to the reduced problem (1.1.2), (1.1.4), (1.1.5), it is possible to prove convergence to an entropy solution by repeating the analysis in Section 5. For Scheme 3, the convergence proof still goes through, but it is not clear that our proof of convergence to an entropy solution (Lemma 5.2) is directly applicable. However, our numerical experiments seem to indicate that approximations generated by Scheme 3 converge to the same (entropy) solutions as provided by Schemes 1 and 2.

7 Numerical results

7.1 Numerical solutions of the reduced problem

In the first series of examples, Cases 1 to 4, we consider the reduced problem (1.1.2), (1.1.4), (1.1.5). We assume that the function $b(u)$ is given by (1.1.6) with $v_\infty = 6.75$, $u_{\max} = 1$ and $n = 2$. The plots of Figure 3 correspond to the parameters given in Table 1. The

Table 1. *Parameters for the numerical examples for the reduced problem shown in Figure 3*

Case	q	$-\gamma_+$	$u_0(x)$	λ
1	−4.9	−4.3	$0.1\chi_{[-2,2]}(x)$	0.03125
2	−2.8	−2.6	$0.1\chi_{[-1,1]}(x)$	0.04
3	−4.9	0	$0.1\chi_{[-2,-0.4]}(x)$	0.04
4	−4.9	−4.9	$0.1\chi_{[-2,-0.4]}(x)$	0.025
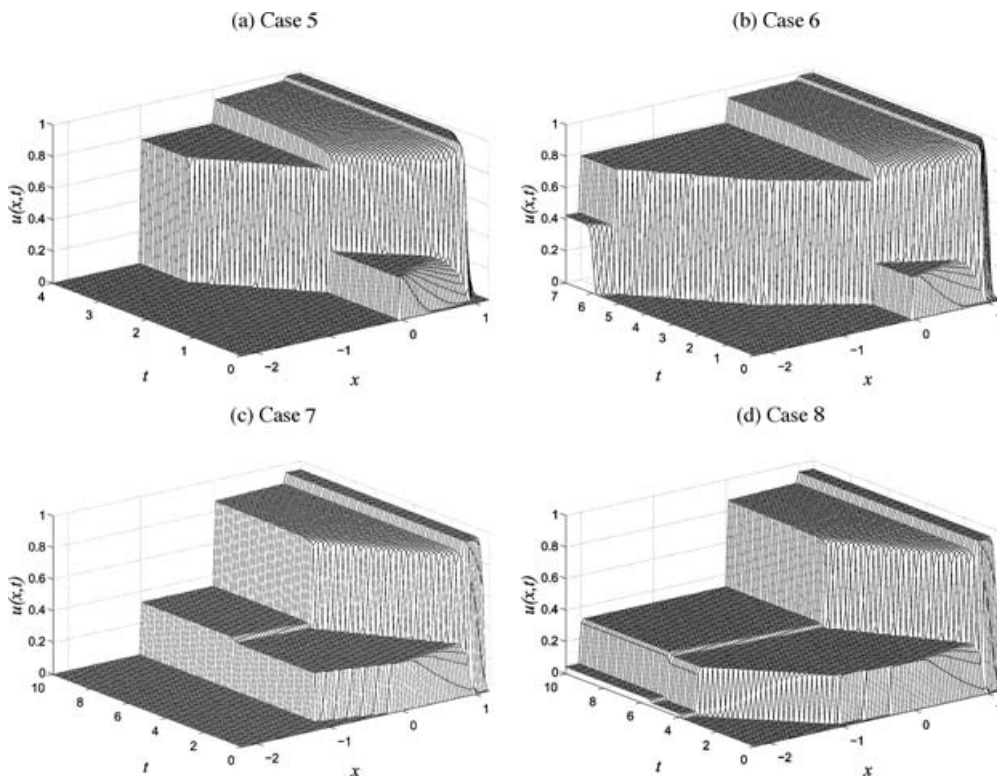
FIGURE 4. Numerical examples with $\Delta x = 0.0125$ for the full extended clarifier-thickener model.

simulations have been made with Scheme 3, $\Delta x = 1/80$, and the values of $\lambda = \Delta t/\Delta x$ indicated in Table 1. Note that the sink term in Case 3 is switched off. This solution of a standard nonlinear conservation law has been included to illustrate the difference to Case 4, where the sink term is included, but all other parameters are the same.

7.2 Numerical solutions of the full problem

Next, we consider the full extended clarifier-thickener model (1.1.1), (1.1.4), (1.1.7)–(1.1.9). The parameters of four different simulations shown in Figure 4, Cases 5 to 8, are shown

Table 2. *Parameters for the numerical examples for the reduced problem shown in*
Figure 4

Case	q_L	q_D	q_R	u_F	λ
5	0.0	−1.0	0.6	0.7	0.05333
6	−0.7	−0.3	0.6	0.7	0.06250
7	−2.25	−2.25	1.35	0.3	0.03922
8	−3.6	−2.25	1.35	0.3	0.03968
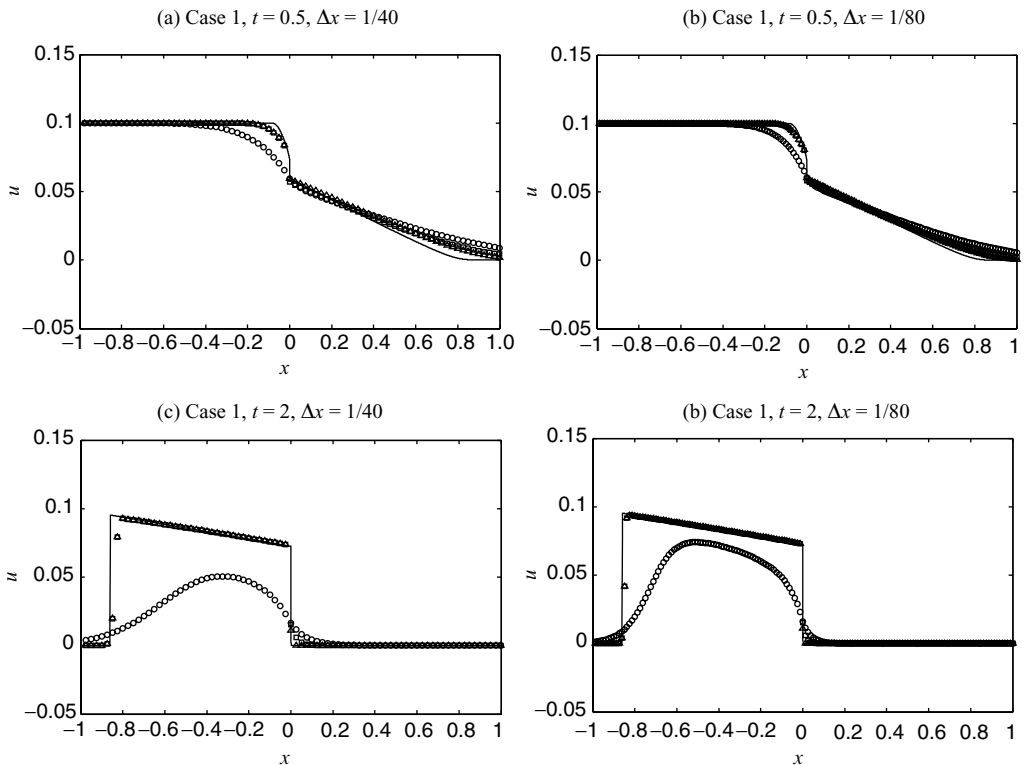
FIGURE 5. Comparison of Scheme 1 ($\bigcirc$), Scheme 2 ($\square$) and Scheme 3 ($\triangle$) applied to Case 1. The solid line is a reference solution with $\Delta x = 1/1600$.

in Table 2. In all cases, we start from an initially empty clarifier-thickener unit ($u_0 \equiv 0$), and consider the same function $b(u)$ as for Cases 1 to 4. The simulations have been made with $\Delta x = 1/80$ and the values of λ given in Table 2.

7.3 Error study

We consider first Case 1, which corresponds to the reduced problem. Figure 5 shows the numerical solution produced by Schemes 1, 2 and 3 for $t = 0.5$ and $t = 2$, while Table 3 displays the approximate L^1 error for this case, measured over the interval $[-1, 1]$.

Table 3. *Approximate L^1 errors for Case 1*

	$t = 0.5$		$t = 2$	
$J = 1/\Delta x$	approx. L^1 error	conv. rate	approx. L^1 error	conv. rate
		Scheme 1		
20	1.715e-2		6.214e-2	
40	1.195e-2	0.522	4.418e-2	0.492
80	8.363e-3	0.515	2.616e-2	0.756
160	5.610e-3	0.576	1.510e-2	0.793
320	3.571e-3	0.652	8.573e-3	0.817
		Scheme 2		
20	7.785e-3		8.310e-3	
40	5.285e-3	0.559	4.332e-3	0.940
80	3.422e-3	0.627	2.221e-3	0.963
160	2.081e-3	0.718	1.107e-3	1.005
320	1.174e-3	0.826	5.171e-4	1.098
		Scheme 3		
20	8.067e-3		7.033e-3	
40	5.045e-3	0.677	3.694e-3	0.929
80	3.003e-3	0.749	1.903e-3	0.957
160	1.674e-3	0.843	9.476e-4	1.006
320	8.487e-4	0.980	4.379e-4	1.114

Next, we consider Case 5, which corresponds to the full problem. Figure 6 shows the numerical solution produced by Schemes 1, 2 and 3 for $t = 1$, $t = 2$ and $t = 4$, respectively, while Table 4 displays the approximate L^1 error for this case, measured over the interval $[-2.1, 1.1]$ (so that all flux discontinuities are included). Finally, we present in Figure 7 numerical solutions generated by all three schemes for Case 7 and $t = 0.3$ and $t = 10$. The corresponding approximate L^1 errors are shown in Table 5.

8 Conclusion

8.1 Discussion of the numerical results

Figure 3 illustrates that the sink term gives rise to a variety of stationary discontinuities. In fact, the reduced problem models how material whose flow is otherwise governed by the conservation law $u_t + \varphi(u)_x = 0$ is absorbed by a singular sink. In Cases 1 and 4, the sink produces a decreasing step (in the direction of increasing x), while in Case 2, an increasing step is generated. Observe that in Case 2, roughly at $t = 2$, the stationary discontinuity at $x = 0$ ceases to exist, and is followed by a curved shock moving in direction of $x > 0$.
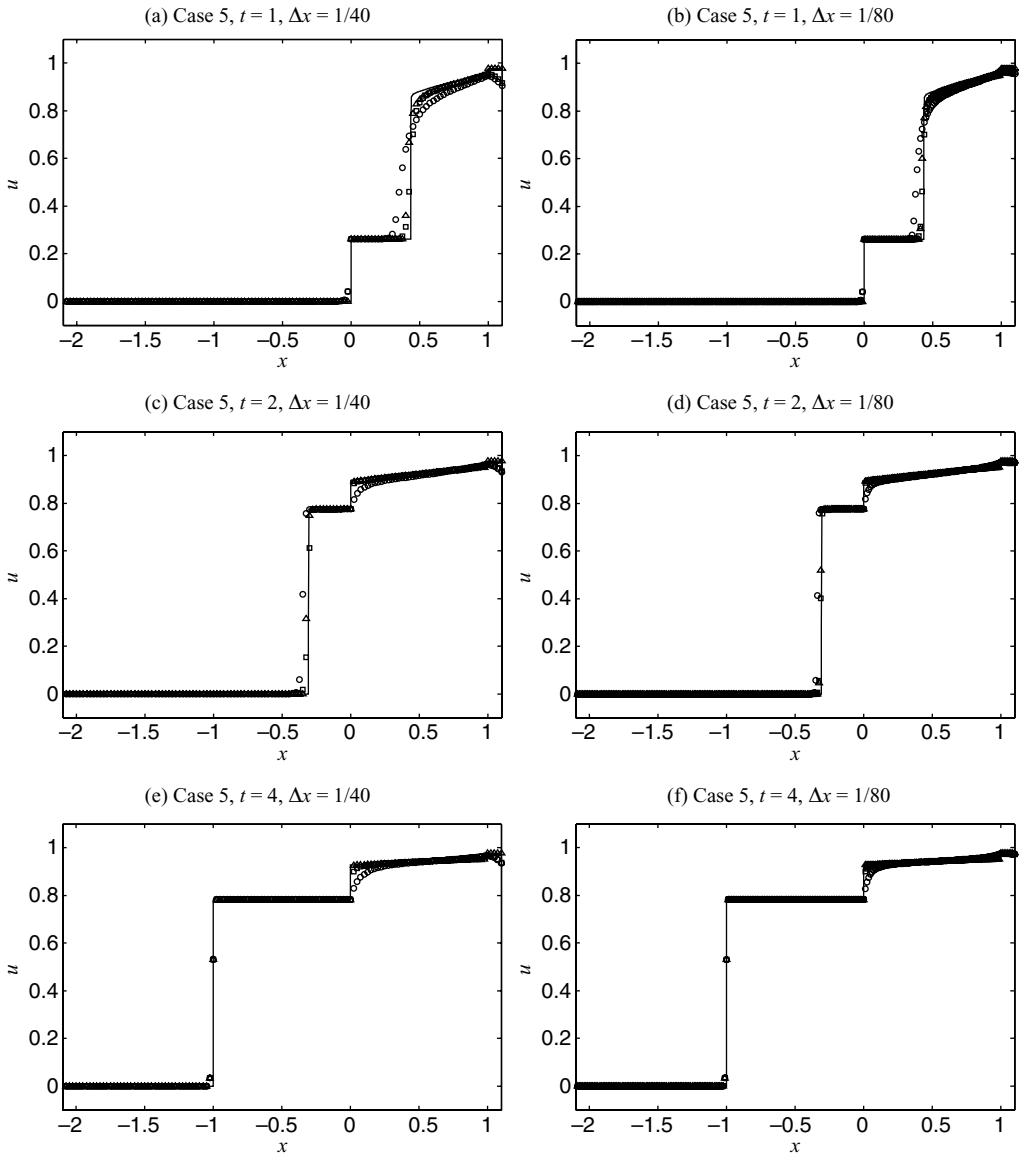
FIGURE 6. Comparison of Scheme 1 (○), Scheme 2 (□) and Scheme 3 (△) applied to Case 5. The solid line is a reference solution with $\Delta x = 1/1600$.

The parameters in Figure 4 have been chosen in such a way that either the solid material flowing into the clarifier zone is fully absorbed by the singular sink term (Cases 5 and 7), or material is extracted through the sink without affecting the solution in the clarifier zone (Cases 6 and 8). The absence of a discontinuity across $x = x_D = -1$ in these cases can be made plausible if we look at the associated reduced problem for the parameters given in these cases. For instance, Case 6 corresponds to $q = q_L = -0.7$. We

Table 4. *Approximate* L^1 *errors for Case 5*

$J = 1/\Delta x$	t = 1		t = 2		t = 4	
	approx. L^1 error	conv. rate	approx. L^1 error	conv. rate	approx. L^1 error	conv. rate
	Scheme 1					
20	1.139e-1		9.123e-2		7.228e-2	
40	6.561e-2	0.796	4.836e-2	0.916	2.739e-2	1.400
80	4.000e-2	0.714	3.178e-2	0.605	1.488e-2	0.880
160	2.587e-2	0.628	2.123e-2	0.582	8.269e-2	0.848
320	1.665e-2	0.636	1.383e-2	0.619	4.521e-3	0.871
	Scheme 2					
20	7.118e-2		6.616e-2		5.614e-2	
40	2.876e-2	1.308	2.201e-2	1.588	1.856e-2	1.597
80	1.268e-2	1.182	1.106e-2	0.994	1.001e-2	0.891
160	7.428e-3	0.771	5.740e-3	0.946	5.577e-3	0.844
320	4.713e-3	0.656	4.111e-3	0.482	3.025e-3	0.882
	Scheme 3					
20	3.483e-2		3.151e-2		2.466e-2	
40	1.990e-2	0.808	1.753e-2	0.846	1.241e-2	0.991
80	1.101e-2	0.854	9.637e-3	0.863	6.164e-3	1.009
160	6.118e-3	0.847	3.984e-3	1.274	2.979e-3	1.049
320	3.128e-3	0.968	1.906e-3	1.064	1.352e-3	1.140

observe in Figure 4 (b) that the solution in the clarification zone after the solids break through the feed level assumes at least a value of 0.78. However, inspecting the shape of $u \mapsto b(u)$ it is easy to see that we have

$$\sup_{u^+ \in [0.78,1]} \max_{u^- \in [0,1]} \frac{\varphi(u^+) - \varphi(u^-)}{u^+ - u^-}$$

$$= q + \sup_{u^+ \in [0.78,1]} \max_{u^- \in [0,1]} \frac{b(u^+) - b(u^-)}{u^+ - u^-}$$

$$\leqslant q + \frac{b(0.78) - b(0)}{0.78} = -0.7 + 6.75 \times 0.22^2 = -0.3733,$$

so for this value and $u_+ \geqslant 0.78$ (in fact, we may choose this lower bound even smaller), the left-hand inequality in jump condition (3.3.9) is never satisfied. In other words, from an engineering point of view, jump condition (3.3.9) helps to predict under which flow conditions extracting material from a sink affects the bulk concentration (i.e. causes a concentration jump) and under which conditions this does not happen (as in our Cases 6 and 8).
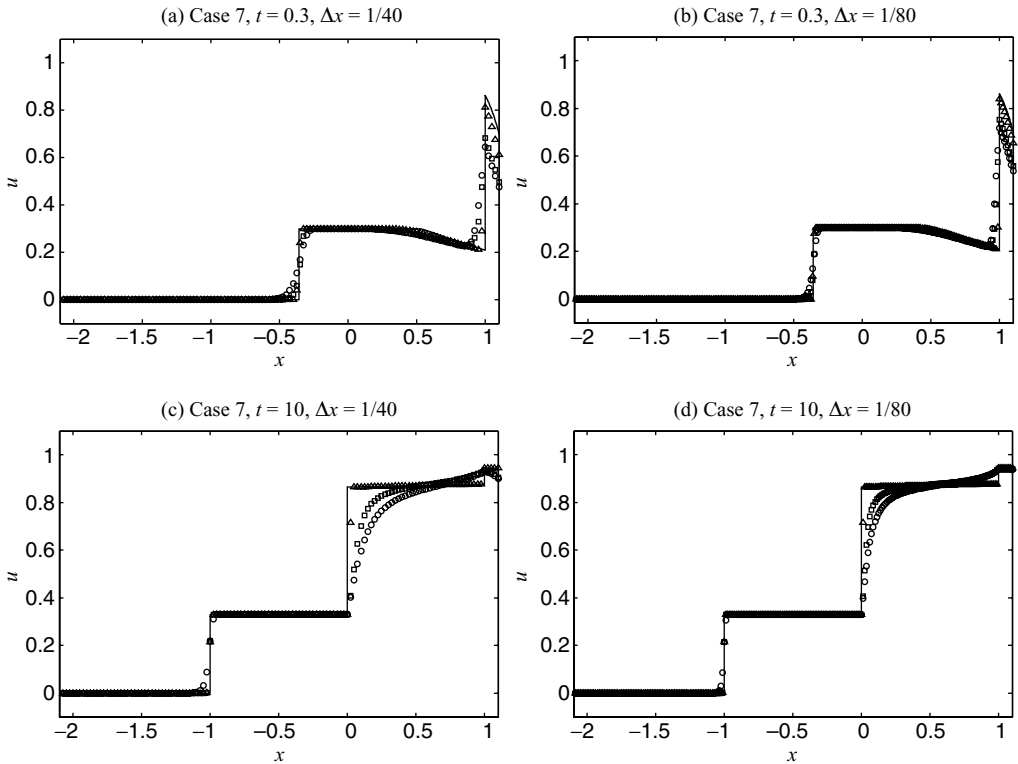
FIGURE 7. Comparison of Scheme 1 (○), Scheme 2 (□) and Scheme 3 (△) applied to Case 7. The solid line is a reference solution with $\Delta x = 1/1600$.

Figures 5 to 7 and Tables 3 to 5 illustrate that all schemes converge to the unique entropy solution of the reduced problem or the full extended clarifier-thickener model. However, all these results also show that Scheme 1, though it has the convenience of being easy to implement, suffers from excessive numerical viscosity, which becomes apparent in smearing of transient shocks travelling at nonzero speed (for example, near $x = 0.5$ in Figures 6 (a) and (b)) and the formation of one-sided boundary layers near discontinuities of the flux function (for example, near $x = 0$ in Figures 7 (c) and (d)). Scheme 2 exhibits smaller numerical viscosity, while Scheme 3 sharply resolves all flux discontinuities. Both Schemes 2 and 3 sharply resolve the solution near $x_{\mathrm{D}} = -1$. Let us comment that the superiority of Scheme 3 is in part balanced by the slightly increased effort needed to evaluate the flux functions h^2 and h^3, which need to be calculated anew (by a discussion of extrema) for each value of the control variables q_{R}, q_{F}, q_{D} and u_{F}.

8.2 Discussion of the entropy condition

From the proof of Lemma 5.2, it is evident that the entropy jump conditions (**D**.3) that hold at the interface ultimately result from the dissipation built into the monotone difference scheme described in Section 4. To be more specific, in the proof of Lemma 5.2 we

Table 5. *Approximate L^1 errors for Case 7*

$J = 1/\Delta x$	$t = 0.3$		$t = 10$	
	approx. L^1 error	conv. rate	approx. L^1 error	conv. rate
			Scheme 1	
20	9.406e-2		1.946e-1	
40	6.394e-2	0.557	1.069e-1	0.864
80	4.255e-2	0.588	6.332e-2	0.756
160	2.685e-2	0.664	3.694e-2	0.778
320	1.609e-2	0.739	2.084e-2	0.826
			Scheme 2	
20	7.619e-2		1.365e-1	
40	5.023e-2	0.601	7.423e-2	0.879
80	3.176e-2	0.661	4.303e-2	0.787
160	1.888e-2	0.751	2.465e-2	0.804
320	1.069e-2	0.821	1.358e-2	0.860
			Scheme 3	
20	3.092e-2		4.109e-2	
40	1.738e-2	0.831	2.041e-2	1.010
80	9.185e-3	0.920	1.000e-2	1.029
160	4.420e-3	1.055	4.766e-3	1.069
320	2.134e-3	1.051	2.131e-3	1.161

employ two different Lipschitz-continuous regularizations, $\bar{\gamma}^\epsilon(x) \geqslant \gamma(x)$ and $\underline{\gamma}^\epsilon(x) \leqslant \gamma(x)$, which approximate the parameter function $\gamma(x)$. Examining that proof, it is clear that the entropy conditions (**D**.3) can be derived by employing monotone schemes for each of the two regularized conservation laws that result by replacing γ by $\bar{\gamma}^\epsilon$ and $\underline{\gamma}^\epsilon$. This yields ϵ-dependent entropy conditions. The entropy conditions (**D**.3) then result by letting the regularization parameter $\epsilon \to 0$.

8.3 An open problem

Using the monotone difference scheme (5.5.1), we have established well-posedness of the reduced model. Our ultimate interest is the more complicated scheme (4.4.2) which we use to construct approximate solutions of the full model. We have focused on the reduced model and its associated scheme in order to highlight the aspects of the problem that are more or less unique to the sink portion of the model. We leave as an open problem the task of combining the definition of entropy solution and the results of the present paper with those of [12]. The goal would be to prove that the version of Theorem 5.1 that applies to the full problem is also true.

Acknowledgements

References

[1] ADIMURTHI & VEERAPPA GOWDA, G.D. (2002) Conservation law with discontinuous flux. *J. Math. Kyoto Univ.*, **42**, 27–70.

[2] AMADORI, D., GOSSE, L. & GUERRA, G. (2004) Godunov-type approximation for a general resonant balance law with large data. *J. Differential Equations*, **198**, 233–274.

[3] AUDUSSE, E. & PERTHAME, B. (2005) Uniqueness for a scalar conservation law with discontinuous flux via adapted entropies. *Proc. Royal Soc. Edinburgh Sect. A*, **135**, 253–265.

[4] BACHMANN, F. & VOVELLE, J. (2006) Existence and uniqueness of entropy solution of scalar conservation laws with a flux function involving discontinuous coefficients. *Comm. Partial Differential Equations*, **31**, 371–395.

[5] BERRES, S., BÜRGER, R., KARLSEN, K. H. & TORY, E. M. (2003) Strongly degenerate parabolic-hyperbolic systems modeling polydisperse sedimentation with compression. *SIAM J. Appl. Math.*, **64**, 41–80.

[6] BERRES, S., BÜRGER, R. & KARLSEN, K.H. (2004) Central schemes and systems of conservation laws with discontinuous coefficients modeling gravity separation of polydisperse suspensions. *J. Comp. Appl. Math.*, **164–165**, 53–80.

[7] BOUCHUT, F. & JAMES, F. (1998) One-dimensional transport equations with discontinuous coefficients. *Nonlinear Anal.*, **32**, 891–933.

[8] BÜRGER, R. & KARLSEN, K.H. (2003) On a diffusively corrected kinematic-wave traffic flow model with changing road surface conditions. *Math. Models Methods Appl. Sci.*, **13**, 1767–1799.

[9] BÜRGER, R., KARLSEN, K. H., KLINGENBERG, C. & RISEBRO, N. H. (2003) A front tracking approach to a model of continuous sedimentation in ideal clarifier-thickener units. *Nonlin. Anal. Real World Appl.*, **4**, 457–481.

[10] BÜRGER, R., KARLSEN, K. H., MISHRA, S. & TOWERS, J. D. (2005) On conservation laws with discontinuous flux. In: Y. Wang and K. Hutter (Eds.), Trends in Applications of Mathematics to Mechanics, Shaker Verlag, Aachen, 75–84.

[11] BÜRGER, R., KARLSEN, K. H., RISEBRO, N. H. & TOWERS, J. D. (2004) Numerical methods for the simulation of continuous sedimentation in ideal clarifier-thickener units. *Int. J. Mineral Process.*, **73**, 209–228.

[12] BÜRGER, R., KARLSEN, K. H., RISEBRO, N. H. & TOWERS, J. D. (2004) Well-posedness in BV_t and convergence of a difference scheme for continuous sedimentation in ideal clarifier-thickener units. *Numer. Math.*, **97**, 25–65.

[13] BÜRGER, R., KARLSEN, K. H. & TOWERS, J. D. (2005) Closed-form and finite difference solutions to a population balance model of grinding mills. *J. Eng. Math.*, **51**, 165–195.

[14] BÜRGER, R., KARLSEN, K. H. & TOWERS, J. D. (2005) A model of continuous sedimentation of flocculated suspensions in clarifier-thickener units. *SIAM J. Appl. Math.*, **65**, 882–940.

[15] BÜRGER, R., KARLSEN, K. H. & TOWERS, J. D. (2005) Mathematical model and numerical simulation of the dynamics of flocculated suspensions in clarifier-thickeners. *Chem. Eng. J.*, **111**, 119–134.

[16] Bustos, M. C., Concha, F., Bürger, R. & Tory, E. M. (1999) *Sedimentation and Thickening*. Kluwer Academic Publishers, Dordrecht, The Netherlands.

[17] Čanić, S. & Mirković, D. (2001) A hyperbolic system of conservation laws in modeling endovascular treatment of abdominal aortic aneurysm. In: Freistühler, H. and Warnecke, G. (eds.), *Hyperbolic Problems: Theory, Numerics, Applications. Eighth International Conference in Magdeburg*, February/March 2000, Volume I. International Series of Numerical Mathematics **140**, Birkhäuser Verlag, Basel, 227–236.

[18] Crandall, M. G. & Majda, A. (1980) Monotone difference approximations for scalar conservation laws. *Math. Comp.*, **34**, 1–21.

[19] Diehl, S. (1995) On scalar conservation laws with point source and discontinuous flux function. *SIAM J. Math. Anal.*, **26**, 1425–1451.

[20] Diehl, S. (1996) A conservation law with point source and discontinuous flux function modelling continuous sedimentation. *SIAM J. Appl. Math.*, **56**, 388–419.

[21] Diehl, S. (1996) Scalar conservation laws with discontinuous flux function: I. The viscous profile condition. *Commun. Math. Phys.*, **176**, 23–44.

[22] Diehl, S. (1997) Dynamic and steady-state behaviour of continuous sedimentation. *SIAM J. Appl. Math.*, **57**, 991–1018.

[23] Diehl, S. (2000) On boundary conditions and solutions for ideal clarifier-thickener units. *Chem. Eng. J.*, **80**, 119–133.

[24] Diehl, S. (2001) Operating charts for continuous sedimentation I: Control of steady states. *J. Eng. Math.*, **41**, 117–144.

[25] Diehl, S. & Wallin, N.-O. (1996) Scalar conservation laws with discontinuous flux function: II. On the stability of the viscous profiles. *Commun. Math. Phys.*, **176**, 45–71.

[26] Engquist, B. & Osher, S. (1981) One-sided difference approximations for nonlinear conservation laws. *Math. Comp.*, **36**, 321–351.

[27] Galvin, K. P., Callen, A., Zhou, J. & Doroodchi, E. (2005) Performance of the reflux classifier for gravity separation at full scale. *Minerals Eng.*, **18**, 19–24.

[28] Galvin, K. P., Doroodchi, E., Callen, A. M., Lambert, N. & Pratten, S. J. (2002) Pilot plant trial of the reflux classifier. *Minerals Eng.*, **15**, 19–25.

[29] Galvin, K. P. & Nguyentranlam, G. (2002) Influence of parallel plates in a liquid fluidized bed system. *Chem. Eng. Sci.*, **57**, 1231–1234.

[30] Gimse, T. (1993) Conservation laws with discontinuous flux functions. *SIAM J. Math. Anal.*, **24**, 279–289.

[31] Gimse, T. & Risebro, N. H. (1992) Solution of the Cauchy problem for a conservation law with a discontinuous flux function. *SIAM J. Math. Anal.*, **23**, 635–648.

[32] Harten, A. (1983) High resolution schemes for hyperbolic conservation laws. *J. Comp. Phys.*, **49**, 357–393.

[33] Kaasschieter, E. F. (1999) Solving the Buckley-Leverett equation with gravity in a heterogeneous porous medium. *Comput. Geosci.*, **3**, 23–48.

[34] Karlsen, K. H., Klingenberg, C. & Risebro, N. H. (2003) A relaxation scheme for conservation laws with a discontinuous coefficient. *Math. Comp.* **73**, 1235–1259.

[35] Karlsen, K. H., Risebro, N. H. & Towers, J. D. (2003) L^1 stability for entropy solutions of nonlinear degenerate parabolic convection-diffusion equations with discontinuous coefficients. *Skr. K. Nor. Vid. Selsk.*, 49 pp.

[36] Karlsen, K. H. & Towers, J. D. (2004) Convergence of the Lax-Friedrichs scheme and stability for conservation laws with a discontinuous space-time dependent flux. *Chin. Ann. Math.*, **25B**, 287–318.

[37] Klausen, R. A. & Risebro, N. H. (1999) Stability of conservation laws with discontinuous coefficients. *J. Diff. Eqns.*, **157**, 41–60.

[38] Klingenberg, C. & Risebro, N. H. (1995) Convex conservation laws with discontinuous coefficients. *Comm. Partial Differential Equations*, **20**, 1959–1990.

[39] Kružkov, S. N. (1970) First order quasilinear equations in several independent variables. *Math. USSR Sb.*, **10**, 217–243.

[40] KYNCH, G. J. (1952) A theory of sedimentation. *Trans. Faraday Soc.*, **48**, 166–176.

[41] MISHRA, S. (2005) Convergence of upwind finite difference schemes for a scalar conservation law with indefinite discontinuities in the flux function. *SIAM J. Numer. Anal.*, **43**, 559–577.

[42] MOCHON, S. (1987) An analysis of the traffic on highways with changing road surface conditions. *Math. Modelling*, **9**, 1–11.

[43] NASR-EL-DIN, H., MASLIYAH, J. H. & NANDAKUMAR, K. (1990) Continuous gravity separation of concentrated bidisperse suspensions in a vertical column. *Chem. Eng. Sci.*, **45**, 849–857.

[44] NASR-EL-DIN, H., MASLIYAH, J. H. & NANDAKUMAR, K. (1999) Continuous separation of suspensions containing light and heavy particle species. *Canad. J. Chem. Eng.*, **77**, 1003–1012.

[45] NASR-EL-DIN, H., MASLIYAH, J. H., NANDAKUMAR, K. & LAW, D. H.-S. (1988) Continuous gravity separation of a bidisperse suspension in a vertical column. *Chem. Eng. Sci.*, **43**, 3225–3234.

[46] NGUYENTRANLAM, G. & GALVIN, K. P. (2001) Particle classification in the reflux classifier. *Minerals Eng.*, **14**, 1081–1091.

[47] OSTROV, D. (2002) Solutions of Hamilton-Jacobi equations and scalar conservation laws with discontinuous space-time dependence, *J. Differential Equations*, **182**, 51–77.

[48] RICHARDSON, J. F. & ZAKI, W. N. (1954) Sedimentation and fluidization: Part I. *Trans. Instn. Chem. Engrs. (London)*, **32**, 35–53.

[49] ROSS, D. S. (1988) Two new moving boundary problems for scalar conservation laws. *Comm. Pure Appl. Math.*, **41**, 725–737.

[50] SEGUIN, N. & VOVELLE, J. (2003) Analysis and approximation of a scalar conservation law with a flux function with discontinuous coefficients. *Math. Models Meth. Appl. Sci.*, **13**, 221–257.

[51] SPANNENBERG, A., GALVIN, K., RAVEN, J. & SCARBORO, M. (1996) Continuous differential sedimentation of a binary suspension. *Chem. Eng. in Australia*, **21**, 7–11.

[52] TOWERS, J. D. (2000) Convergence of a difference scheme for conservation laws with a discontinuous flux. *SIAM J. Numer. Anal.*, **38**, 681–698.

[53] TOWERS, J. D. (2001) A difference scheme for conservation laws with a discontinuous flux: The nonconvex case. *SIAM J. Numer. Anal.*, **39**, 1197–1218.

[54] VAN DUIJN, C. J., DE NEEF, M. J. & MOLENAAR, J. (1995) Effects of capillary forces on immiscible two-phase flow in strongly hetereogeneous porous media. *Transp. Porous Media*, **21**, 71–93.